Oral vancomycin treatment alters serum levels of indole derivatives and secondary bile acids modulating the expression of mTOR pathway genes in astrocytes during EAE

Paola Bianchimano[a,b,c,1], Paola Leone[a,b,c,1], Emma M. Smith[a,b,c], Cristina Gutierrez-Vazquez[d], Erli Wind-andersen[c,e], Gerold Bongers[c], Sebastian Cristancho[a,b,c], Howard L. Weiner[d], Jose C. Clemente[c,e] and Stephanie K. Tankou[a,b,c,*]

[a] Department of Neurology, Icahn School of Medicine at Mount Sinai, New York, NY, USA
[b] Friedman Brain Institute, Icahn School of Medicine at Mount Sinai, New York, NY, USA
[c] Precision Immunology Institute, Icahn School of Medicine at Mount Sinai, New York, NY, USA
[d] Ann Romney Center for Neurologic Diseases, Harvard Medical School, Brigham and Women's Hospital, Boston, MA
[e] Dept of Genetics and Genomic Sciences, Icahn School of Medicine at Mount Sinai, New York, NY, USA
[1] These authors contributed equally
*Corresponding author at: 5E 98th Street, 1st Floor, New York, NY 10029, USA
E-mail address: stephanie.tankou@mssm.edu

HIGHLIGHTS

- Vancomycin attenuated established EAE through regulation of the microbiota.
- Vancomycin induced increased serum level of indole-3-lactic acid as well as decreased serum levels of indoxyl-3-sulfate, p-cresol and deoxycholic acid.
- Vancomycin modulated the expression of mTOR pathway genes in astrocytes
- *Lactobacillus reuteri* (enriched in vancomycin treated mice) regulated the expression of mTOR pathway genes in astrocytes
- Serum levels of indole-3-lactic acid, indoxyl-3-sulfate, p-cresol and deoxycholic acid correlated with expression of mTOR pathway genes in astrocytes

ABSTRACT

Astrocytes play important roles in the central nervous system (CNS) during health and disease. Prior studies have shown that gut commensals derived indole derivatives as well as secondary bile acids modulate astrocyte function during the late stage of EAE (recovery phase). Here we show that administering vancomycin to mice starting during the early stage of EAE improved disease recovery, an effect that is mediated by the gut microbiota. We observed that 6 taxa within the *Clostridia vadinBB60* genus were enriched in vancomycin treated mice compared to untreated EAE mice. Vancomycin-treated EAE mice also had elevated serum levels of the anti-inflammatory tryptophan derived metabolite, indole-3-lactic acid and decreased levels of deoxycholic acid, a pro-inflammatory secondary bile acid. RNA sequencing revealed altered expression of several genes belonging to the mammalian target of rapamycin (mTOR) pathway in astrocytes obtained during the late stage of EAE from vancomycin treated EAE mice. Furthermore, we observed a link between serum levels of indole derivatives and bile acids and expression of several genes belonging to the mTOR pathway. Interestingly, the mTOR signaling cascades have been implicated in several key biological processes including innate (e.g., astrocyte) immune responses as well as neuronal toxicity/degeneration. In addition, rapamycin, a specific inhibitor of mTOR, has been shown to inhibit the induction and progression of established EAE. Collectively, our findings suggest that the neuroprotective effect of vancomycin is at least partially mediated by indole derivatives and secondary bile acids modulating the expression of mTOR pathway genes in astrocytes.

INTRODUCTION

Multiple sclerosis (MS) is a chronic central nervous system (CNS) inflammatory and neurodegenerative disease and one of the leading causes of disability in young individuals. MS is typically diagnosed between the ages of 20-40 as relapsing-remitting MS and 15-20 years later, some of these patients are going to enter the progressive phase of the disease which is non-remitting. Several

drugs are FDA approved for the treatment of MS and are effective at suppressing relapsing disease but have limited impact on disease progression. During the progressive phase of MS, the inflammatory response is confined to the CNS and is primarily driven by astrocytes and microglia[1,2]. Astrocytes are the most abundant cell population in the CNS, and they have several functions including modulation of the blood-brain barrier, regulation of neuronal transmission and CNS development and repair[3–6]. Astrocytes have also been implicated in the pathogenesis of several CNS inflammatory and neurodegenerative diseases including MS and its mouse model[7–10]. One possible reason why the current immunomodulatory therapies failed in progressive MS is because they do not effectively target astrocytes or microglia. Hence, developing novel disease modifying therapeutic strategies is crucial to slowing cognitive decline and enhancing the quality of life of progressive MS patients.

The gut microbiome plays an important role in autoimmunity including MS and its mouse model, experimental autoimmune encephalomyelitis (EAE)[11–14]. One study reported that dietary tryptophan is metabolized by the gut microbiota into indole and its derivatives which are aryl hydrocarbon receptor (AhR) agonists acting on astrocytes to limit CNS inflammation and neurodegeneration in EAE mice[15]. The same study found that oral administration of ampicillin but not vancomycin during the late stage of EAE interfered with disease recovery by modulating astrocyte function via alteration in gut derived AhR agonists levels namely, indole-3-propionic acid, indoxyl-3-sulfate and indole-3-aldehyde[15]. Hence, indole derivatives are important regulators of the gut-brain axis during EAE. While human MS differs in many ways from EAE, multiple MS-associated microorganisms exacerbate the EAE phenotype and EAE mice colonized with MS derived microbiota develop more severe disease than EAE mice reconstituted with healthy donor derived microbiota. These findings demonstrate that aspects of EAE reflect clinically relevant host-microbiome interactions, providing mechanistic insights essential to interpret the large-scale studies correlating aspects of the gut microbiome with MS in patients.

The identity of gut commensals modulating astrocyte function remains obscure. We have previously shown that oral administration of vancomycin prior to EAE induction ameliorates disease and demonstrated that this protective effect is mediated via the microbiota[13]. In the present study, we showed that EAE mice fed microbiota derived from vancomycin treated mice post-symptoms onset had better recovery than mice fed microbiota from untreated mice. We observed that administration of vancomycin post-EAE induction but before symptoms onset (early stage of EAE) improved disease recovery. Microbiome characterization sequencing revealed enrichment of the genus *Clostridia vadinBB60 group* in vancomycin treated EAE mice. Vancomycin and ampicillin treated mice had decreased serum levels of indoxyl-3-sulfate (3-IS), indole-3-propionic acid (3-IPA) and p-cresol compared to untreated EAE mice. Vancomycin but not ampicillin treated EAE mice had increased serum indole-3-lactic acid (3-ILA) levels compared to untreated EAE mice. Interestingly, we observed a positive correlation between serum level of ILA and the abundance of 4 taxa belonging to *Clostridia vadinBB60 group* genus. We also found decreased serum levels of most secondary bile acids including deoxycholic acid (DCA), a pro-inflammatory bile acid, in vancomycin treated EAE mice. Serum level of DCA positively correlated with the abundance of 6 taxa belonging to *Muribaculaceae* genus which was enriched in untreated EAE mice compared to vancomycin treated EAE mice.

Given that indole and its derivatives are AhR agonists that have been shown to modulate astrocyte function during EAE, we conducted RNA sequencing on astrocytes derived from these EAE mice. RNA sequencing of astrocytes revealed that vancomycin altered the expression of multiple genes including genes belonging to the mTOR pathway. We observed a correlation between levels of expression of genes belonging to the mTOR pathway in astrocytes and serum levels of indole derivatives and bile acids. Furthermore, we have previously observed increased abundance of *Lactobacillus reuteri*, an indole-3-lactic acid producing bacteria, in vancomycin treated mice. In the current study, we found increased abundance of *Lactobacillus reuteri* in vancomycin treated naïve mice. We showed that mice supplemented with *L. reuteri* prior to EAE induction or at the time of symptoms onset had better disease recovery compared to EAE mice who received vehicle. We also performed RNA sequencing from astrocytes isolated from mice receiving *L. reuteri* or vehicle. We observed alteration in the expression of genes belonging to the mTOR pathway including increased expression of Acsl3 in mice supplemented with *L. reuteri* which was also increased in vancomycin

treated EAE mice. Interestingly, rapamycin, a specific inhibitor of the mTOR pathway ameliorates EAE by inducing T regulatory cells or suppressing Th1 and/or Th17 cells. However, the role of the mTOR pathway in astrocytes during EAE remains poorly understood.

Our results suggest that mTOR pathway genes in astrocytes could be potential targets for therapeutic manipulation and provide a foundation to explore the mechanisms by which gut commensals derived metabolites modulate this pathway in astrocytes during chronic CNS inflammation.

MATERIALS AND METHODS

Mice

C57BL/6J female mice of 8-10 weeks of age were purchased from the Jackson Laboratory and housed in a specific pathogen-free facility at the Icahn School of Medicine at Mount Sinai or the Harvard Institute of Medicine. Animals were kept on a 12-h light/dark cycle with access to food (PicoLab Rodent Diet 5053) and distilled water at neutral pH provided by the animal facility.

Mice were co-housed, 3-5 mice per cage from the same experimental condition. Animals were allowed to acclimate for a total of 5 days before initiation of treatment. Upon arrival at the animal facility, mice were housed in groups of 3-5 per cage by the mice facility staff. Two days after arrival, mice are re-grouped so that each experimental group receives mice from all the cages that were set up on arrival. At this age, mice have not undergone any experimental manipulations and are indistinguishable from one another. Groups are formed by redistributing the mice and exchanging bedding.

Animals were housed in a biosafety level 2 facility using autoclaved cages and aseptic handling procedures. All animal experiments were approved by the Institutional Animal Care and Use Committee (IACUC) at Icahn School of Medicine at Mount Sinai or Harvard Medical School and carried out in accordance with those approved animal experiment guidelines.

EAE induction

EAE was induced in 8- to 10-week-old female C57BL/6J mice by injecting 250 μg of MOG_{35-55} peptide (Genemed Synthesis) emulsified in complete Freund's adjuvant (CFA) (BD Difco) per mouse, injected subcutaneously into each flank, followed by intraperitoneal administration of 150 ng of pertussis toxin (List Biological Laboratories, Inc.) per mouse on day 0. A second dose of 300 ng pertussis toxin was administered on day 2. Clinical signs of EAE were assessed according to the following scale: 0, no signs of disease; 1, loss of tone in the tail; 2, hind limb paresis; 3, hind limb paralysis; 4, tetraplegia; and 5, moribund. Differences between the groups were determined by Friedman test and Dunn's correction for multiple comparisons.

Antibiotic treatments

Vancomycin 0.5mg/mL (Research Products International Corp.) or ampicillin 1mg/ml (Research Products International Corp.) were administered in drinking water. For experiments assessing the impact of the time of initiation of vancomycin treatment on EAE development (Figure 1A), three treatment groups were subjected to different time courses of vancomycin administration: -14 to 0 days post immunization (DPI) (vanco prior), 10 to 30 DPI (vanco post), -14 to 30 DPI (vanco continuous). For experiments characterizing the effects of vancomycin and ampicillin on EAE development (Figure 2A), antibiotics were administered from day 9 post immunization until the end of the experiment.

Fecal microbiota transplantation

Donor mice received either vancomycin 0.5 mg/mL in drinking water or normal drinking water for 2 weeks. Two weeks post vancomycin initiation, ceca were collected under aseptic conditions and processed in an anaerobic chamber to preserve the viability of intestinal bacteria. The content of 1 cecum from vancomycin treated mice, or 3 ceca from control mice were transferred to pre-reduced and anaerobically sterilized PBS (Anaerobe Systems Cat. no. AS-908) and homogenized by vortexing at room temperature. The fecal homogenates were freshly prepared on the day of first gavage. Remaining

fecal slurries were aliquoted, stored at -80°C, and thawed only once for subsequent gavages. Recipient C57BL/6J mice were gavaged 200 µL of the control- or vancomycin- cecal content homogenate 3 times per week starting at day 15 post EAE induction until the end of the experiment.

Lactobacillus reuteri culture and administration

Lactobacillus reuteri, strain CF48-3A (Cat#: HM-102; Biodefense and Emerging Infections Research Resources Repository) was grown in anaerobic conditions at 37 °C in brain-heart infusion (BHI) medium (Cat #: DF0037178; Fisher Scientific). Bacterial cultures were grown for 48-72 hours, centrifugated and resuspended in anaerobic sterile PBS to obtain a suspension of live bacteria at a density of OD600 = 1.3. Mice were administered 200 µL of bacteria suspension via oral gavage 3 times a week beginning either 3 weeks prior to EAE induction or 16 days post MOG immunization, until the end of the experiment. Control mice for this experiment received sterile anaerobic PBS (vehicle) via oral gavage.

Blood collection

Mice were restrained manually by scruffing the skin of the dorsal neck. A 5mm lancet (Fisher, Cat# NC9891620) was used to puncture the facial vein on the right side of the face. Blood was allowed to drip freely into a microtainer tube blood collection with lithium heparin (Fisher, Cat#13-680-62). Hemostasis was achieved by using clean, dry gauze applied directly to the access site. Plasma was separated from cellular fraction by centrifugation and subsequently stored in a -80°C freezer.

Tissue collection

Immediately after blood collection, mice were anesthetized with 5% isoflurane and intracardially perfused through the left ventricle with ice-cold HBSS. Spleens, spinal cords, distal colons and ceca were removed and processed immediately or stored in conditions appropriate for downstream applications. Ceca and distal colon were snap frozen and stored at -80°C for metabolomics and 16S rRNA gene sequencing respectively. Spleens were collected for total CD4 T cells isolation and spinal cords were collected in ice cold HBSS for astrocytes isolation.

16S rRNA gene sequencing and analysis

Distal colons were collected as described above. Bacterial DNA was isolated from distal colons using MoBio PowerLyzer PowerSoil Kit (Qiagen). DNA concentration was quantified using the Quant-iT dsDNA Assay Kit, broad range (Life Technologies) and normalized to 2 ng/µl on a Beckman handling robot. Amplicon preparation and sequencing was performed as previously described[16]. Briefly, bacterial 16S rDNA PCR including no template controls were set up in a separate PCR workstation using dual-indexed primers. PCR reactions contained 1 µM for each primer, 4 ng DNA, and Phusion Flash High-Fidelity PCR Master Mix (Thermo Fisher Scientific). Reactions were held at 98°C for 30 s, proceeding to 50 cycles at 98°C for 10 s, 45°C for 30 s, and 72°C for 30 s and a final extension of 2 min at 72°C. Amplicons were evaluated by gel electrophoresis. The sequencing library was prepared by combining equivolume amounts of each amplicon, size-selected and concentrated using AMPure XP beads (0.8X, Beckman). Library concentration was quantified by Qubit and qPCR, mixed with 15% PhiX, diluted to 4 pM and subjected to paired-end sequencing (Reagent Kit V2, 2x150bp) on an Illumina MiSeq sequencer. Taxonomy was assigned using the Scikit-learn classifier[17] pre-trained on the Silva 132 99% OTUs 515-806 region (silva-132-99-515-806-nb-classifier). Taxonomy summary plots were generated based on relative abundance at the genus level. Beta diversity was estimated using Bray-Curtis, and distances were then used to perform principal coordinate analysis as implemented in QIIME. Differences in beta diversity were tested using PERMANOVA with FDR correction for multiple comparison testing. Compositional differences in the microbiome were determined using a Two-way ANOVA with false discovery rate.

Metabolomics
Ceca and plasma samples were shipped to Metabolon, Inc. (Morrisville, NC) for the targeted analysis of bile acids and dietary tryptophan and tyrosine derived metabolites, respectively. Metabolite levels were analyzed using a liquid chromatography-tandem mass spectrometry (LC-MS/MS) system (Agilent 1290 UHPLC/Sciex QTrap 5500).

Isolation of astrocytes from adult mouse spinal cord
Astrocytes were sorted as previously described[15] and outlined in Supplementary Fig. 4. Briefly, spinal cords were subjected to homogenization using a tissue homogenizer. Subsequently, cells were pelleted and resuspended in 70% Percoll. An overlay of 37% Percoll was then added on top of 70% Percoll and cells mixture, after which samples were centrifuged 30 minutes at 800 G at 25 °C. Mononuclear CNS cells were collected from the 70–30% interphase, further centrifuged and resuspended in FACS buffer (HBSS + 2% FBS + 1M HEPES + 0.5M EDTA). Samples were incubated with anti-mouse CD32 for 5 min at 4°C to block Fc receptors and stained with fluorochrome conjugated antibodies to CD45R/B220 PE (1:200) (clone RA3-6B2, BD Bioscience #553089), Ter119 PE (1:200) (Biolegend #116207), Olig4 PE (1:200) (R&D Systems #FAB1326P), CD105 PE (1:200) (clone MJ7/18, Invitrogen #12105182), CD140a PE (1:200) (clone APA5, Invitrogen #12140181), Ly6G PE (1:200) (clone 1A8, Biolegend #127608), CD11b PE-Cy7 (1:200) (clone M1/70, BD Bioscience #561098), Ly6C PerCp (1:200) (clone HK1.4, Biolegend #128028), CD45 APC (1:200) (clone 30-F11, Invitrogen #17045183), CD11c APC-Cy7 (1:200) (clone HL3, BD Bioscience #561241) for 20 minutes at 4°C in the dark. After staining, cells were washed and incubated with 7-AAD viability dye (Biolegend #420403) for 20 minutes at 4°C in the dark to exclude dead cells. Following additional washes, cells were resuspended in FACS buffer and astrocytes were sorted using a BD CSM5L sorter after negative selection of B cells, T/NK cell subset, erythroid cells, oligodendrocytes, endothelial cells, mesenchymal cells, monocytes, granulocytes, neutrophils, microglia, hematolymphoid cells, dendritic cells.

Bulk RNA sequencing

Antibiotics study. Ultra-low input RNA-seq library preparation, HiSeq sequencing and analysis were conducted at Azenta US, Inc (South Plainfield, NJ, USA). Ultra-low input RNA sequencing library was prepared by using SMART-Seq HT kit for full-length cDNA synthesis and amplification (Takara, San Jose, CA, USA), and Illumina Nextera XT (Illumina, San Diego, CA, USA) library was used for sequencing library preparation. Briefly, cDNA was fragmented, and an adaptor was added using Transposase, followed by limited-cycle PCR to enrich and add index to the cDNA fragments. The sequencing library was validated on the Agilent TapeStation (Agilent Technologies, Palo Alto, CA, USA), and quantified by using Qubit 2.0 Fluorometer (ThermoFisher Scientific, Waltham, MA, USA) as well as by quantitative PCR (KAPA Biosystems, Wilmington, MA, USA). The sequencing libraries were multiplexed and clustered on a flowcell. After clustering, the flowcell was loaded on the Illumina HiSeq instrument according to the manufacturer's instructions. The samples were sequenced using a 2x150 Paired End (PE) configuration. Image analysis and base calling were conducted by the HiSeq Control Software (HCS). Raw sequence data (.bcl files) generated from Illumina HiSeq was converted into fastq files and de-multiplexed using Illumina's bcl2fastq 2.17 software. One mis-match was allowed for index sequence identification. After investigating the quality of the raw data, sequence reads were trimmed to remove possible adapter sequences and nucleotides with poor quality using Trimmomatic v.0.36. The trimmed reads were mapped to the Homo sapiens reference genome available on ENSEMBL using the STAR aligner v.2.5.2b. BAM files were generated as a result of this step. Unique gene hit counts were calculated by using feature Counts from the Subread package v.1.5.2. Only unique reads that fell within exon regions were counted.
After extraction of gene hit counts, the gene hit counts table was used for downstream differential expression analysis. Using DESeq2, a comparison of gene expression between the groups of samples was performed. The Wald test was used to generate P values and Log2 fold changes. Genes with

adjusted P-values < 0.05 and absolute log2 fold changes >1 were considered differentially expressed genes for each comparison.

***Lactobacillus* study**. Ultra-low input RNA-seq library preparation and sequencing reactions were conducted at the Broad Institute (Cambridge, MA, USA) as previously described[18] . Demultiplexed fastq files reflecting RNA-seq data were trimmed for low quality using Trimmomatic[19] and filtered for artificial adapter sequences, followed by application of STAR[20] for alignment to the reference mouse transcriptome (vGRCm38) and gene level quantification using RSEM[21]. Normalization of gene abundance profiles across the sample set was performed using DE-Seq2[22], followed by differential expression analysis of gene families (Wald Test with False Discovery Rate p-value adjustment) to identify differentially expressed genes between groups of interest.

Quantitative PCR

Total CD4 T cells were isolated from spleens using CD4 beads from Miltenyi (Cat# 130-117-043, Miltenyi). Total RNA was isolated from CD4 T cells using the PicoPure RNA extraction kit (Cat# KIT0204, Thermo Fisher) following manufacturer's instructions. First strand cDNA synthesis was performed for each RNA sample for up to 1ug of total RNA using a High-Capacity cDNA Reverse Transcription kit (Fisher, Cat# 4374966). Quantitative PCR (qPCR) analysis was performed in an Applied Biosystems ViiA 7 system (Applied Biosystems), using the SYBR Green master mix and specific primers for IL17A (FWD: agcaagagatcctggtcctgaa, RV: catcttctcgaccctgaaagtga), IL10 (FWD:agaagcatggccctgaaatcaagg RV: cttgtagacaccttggtcttggag), and IFN-g (FWD: gccatcagcaacaacataagcgtc, RV: ccactcggatgagctcattgaatg). GAPDH (FWD: ACAGTCCATGCCATCACTGCC, RV: GCCTGCTTCACCACCTTCTTG) was used as endogenous control to normalize for differences in the amount of total RNA across samples. The relative gene expression was calculated using the comparative CT method[23].

Quantification and statistical analysis

Spearman's rank correlation coefficient was calculated across pairwise elements in different partitions using the spearman r function from the stat module in ScipPy. p-values were corrected for experiments of interest using Python's False-Discovery Rate Benjamini-Hochberg (FDR-BH) function from the statsmodels package. All graphs and additional statistical analyses were performed using the GraphPad Prism software (GraphPad Software, San Diego, CA, USA). Mann-Whitney test was used for comparisons between two groups. Kruskal-Wallis followed by Dunn's test was used for comparisons between 3 or more groups. EAE clinical scores were analyzed over time with the nonparametric Friedman test with Dunn's correction for multiple comparisons. Details about the statistical tests, sample sizes, and p-values are indicated in each figure.

RESULTS

Vancomycin effect on EAE development depends on time of administration

One study showed that administration of vancomycin during the late stage of EAE had no effect on disease severity or recovery[15]. We have previously reported that administration of vancomycin for 2 weeks prior to EAE induction ameliorates EAE[13]. To examine if this apparent discrepancy of vancomycin effect on EAE development from these two studies is due to difference in timing of administration, we next conducted experiments to investigate how the timing and length of administration of vancomycin affect EAE progression. C57BL/6J (B6) EAE mice were administered vancomycin at various time points spanning pre- and post- EAE induction (**Fig 1A**). We observed that mice receiving vancomycin continuously starting at 2 weeks prior to EAE induction (purple group) did not develop disease (**Fig 1A**). Mice who were treated with vancomycin daily for 2 weeks (green group) prior to EAE induction developed mild disease consistent with our prior study[13] (**Fig 1A**). Mice who received vancomycin daily starting at the time of symptoms onset (day 10 post immunization; blue group) developed disease severity that was comparable to that seen in untreated mice (black group)

but had better disease recovery that was similar to that seen in mice treated with vancomycin prior to EAE induction (**Fig 1A**). Hence, vancomycin can both prevent and treat disease in EAE mice. We have shown that germ-free mice colonized with microbiota from vancomycin treated mice developed less severe disease than mice colonized with microbiota from conventionally raised mice[13]. To determine if the microbiota derived from vancomycin treated mice can attenuate established EAE, EAE mice either received microbiota from untreated mice or vancomycin treated mice daily starting at day 15 post immunization (after symptoms onset). We found that mice fed microbiota from vancomycin treated mice had better disease recovery than mice fed microbiota from conventionally raised mice (**Fig 1B**). Hence, the neuroprotective effects of vancomycin are mediated via the microbiota. Taken together, our results revealed that vancomycin neuroprotective effects depend on the length and timing of administration.

Taxa belonging to Clostridia vadinBB60 group genus* are enriched in *mice treated with vancomycin during the late stage of EAE

As mentioned above, gut commensals derived from vancomycin treated mice ameliorate disease recovery in EAE mice. Hence, to identify bacteria modulating disease recovery during EAE, we conducted 16S rRNA gene sequencing to investigate the gut microbiota composition during the late stage of EAE in untreated, vancomycin and ampicillin treated EAE mice. EAE was induced in B6 mice via MOG immunization and at day 9 post immunization (pre-symptoms onset; early stage EAE) these EAE mice were divided in the following 3 groups: 1 group was administered vancomycin once daily, the second group received ampicillin once daily and the third group received vehicle once daily via oral gavage until the end of the experiment. As expected, we found that vancomycin mice had better recovery than the untreated EAE mice (**Fig 2A**). Ampicillin treated EAE mice had delayed symptoms onset compared to untreated and vancomycin treated mice and displayed better disease recovery than untreated EAE mice (**Fig 2A**). At day 23 (late stage EAE), mice were sacrificed, and stool samples were used for 16S rRNA gene sequencing. PCoA plots revealed that the untreated, vancomycin and ampicillin treated EAE mice have a distinct microbiota composition ($q<0.01$ for all pairwise comparisons; **Fig 2B**). We observed increased abundance of *Muribaculaceae*, *LachnospiraceaeNK4A136 group*, *Bacteroides* and *Turicibacter* genera in untreated EAE mice compared to vancomycin and ampicillin treated EAE mice (**Fig 2C-E**). We found that six taxa belonging to *Clostridia vadinBB60 group*, *Enterobacteriaceae*, *Akkermansia*, *Parasuterella* and *Anaeroplasma* genera were enriched in vancomycin treated mice compared to untreated and ampicillin treated EAE mice (**Fig 2C-E**). Interestingly, the genus *Muribaculaceae* has been shown to positively correlate with serum level of the pro-inflammatory cytokine IL-1β[24]. Furthermore, we have previously shown that *Akkermansia* ameliorates EAE[12,25]. Interestingly, a study reported that *Clostridia vadinBB60 group* genus is depleted in treatment naïve MS patients compared to treated MS patients and healthy controls[26]. Hence, our findings suggest that vancomycin administration post EAE induction leads to the depletion of pro-inflammatory bacteria and proliferation of neuroprotective bacteria with a predominance of taxa belonging to *Clostridia vadinBB60 group* genus.

Vancomycin alters metabolism of bile acids, tryptophan and tyrosine derived metabolites during the late stage of EAE

As mentioned above, we found that vancomycin treatment of EAE mice induced significant change in the gut microbiota composition leading to improved disease recovery. A prior study reported that vancomycin-resistant bacteria are indole-producers and that 3 indole derivatives namely, indole-3-propionic acid (3-IPA), indoxyl-3-sulfate (3-IS) and indole-3-aldehyde, are important modulators of the inflammatory response during the recovery phase of EAE[15]. Hence, we next performed serum metabolomics to assess if vancomycin induced changes in the gut microbiota composition are linked to change in serum levels of indole derivatives. We found decreased serum levels of 3-IS, 3-IPA in vancomycin and ampicillin treated naïve and EAE mice compare to untreated naïve and EAE mice (**Fig 3A-B**). We observed increased serum level of 3-IPA in untreated EAE mice compared to untreated naïve mice (**Fig 3B**). Vancomycin treated EAE mice had increased serum 3-IS level compared to

vancomycin treated naïve mice as well as ampicillin treated mice (**Fig 3B-C**). 3-ILA level was comparable in untreated, vancomycin and ampicillin treated naïve mice (**Fig 3A**). We observed increased serum level of 3-ILA in vancomycin treated EAE mice compare to vancomycin treated naïve mice as well as untreated and ampicillin treated EAE mice (**Fig 3A-C**). Serum tryptophan levels were not affected by antibiotic treatment or EAE induction (**Fig 3A-C**). Hence, our results showed that vancomycin depleted bacteria producing 3-IS, 3-IPA but promoted the proliferation of bacteria producing 3-ILA. Interestingly, a prior study reported that high salt diet exacerbates EAE at least in part by inducing the depletion of 3-ILA producing Lactobacillus species[27]. In addition, another study reported that ILA ameliorates EAE[28]. Consistent with our findings, one study observed increased level of 3-IS in the cerebrospinal fluid of untreated MS patients compared to treated MS patients and they found that 3-IS is neurotoxic[29].

In addition to tryptophan derived metabolites, tyrosine derived metabolites, p-cresol and 4-EPS, have been implicated in MS/EAE[29,30] and impaired neuronal myelination[31,32]. Hence, we also examined the effect of vancomycin on serum levels of p-cresol and 4-EPS in our mice. We found decreased serum levels of p-cresol in vancomycin and ampicillin treated naïve and EAE mice compare to untreated naïve and EAE mice (**Fig 3D**). We observed increased serum level of p-cresol in untreated EAE mice compared to untreated naïve mice (**Fig 3E**). 4-EPS serum level was comparable in untreated, vancomycin and ampicillin treated naïve mice (**Fig 3D**). 4-EPS serum level was increased in vancomycin treated EAE mice compared to vancomycin treated naïve mice as well as untreated and ampicillin treated EAE mice (**Fig 3D-F**). Prior studies have shown that p-cresol is pro-inflammatory and neurotoxic[29,33]. Consistent with these findings, we observed that vancomycin depleted gut commensals producing p-cresol. Taken together, our findings suggest that a putative mechanism by which vancomycin ameliorates disease recovery in EAE mice is via inducing the proliferation of anti-inflammatory 3-ILA producing bacteria and depleting bacteria producing neurotoxins 3-IS and p-cresol.

Another study reported altered level of primary and secondary bile acids in MS patients[34]. That same study also reported that supplementation of EAE mice with the secondary acid metabolite, TUDCA, ameliorate disease by modulating glial cells function during the recovery phase. Hence, we next examined the effect of vancomycin on serum levels of bile acids. We found that mice treated with vancomycin or ampicillin had very low serum level of most primary bile acids compared to untreated mice (**Fig 3G-I, Fig S1A-C**). Vancomycin and ampicillin treated naïve mice had increased serum levels of primary bile acids TaMCA, TbMCA and TCA compared to untreated naïve mice (**Fig 3G-H**). Serum levels of TaMCA, TbMCA and TCA were decreased in vancomycin treated EAE mice compared to vancomycin treated naïve mice and ampicillin treated EAE mice (**Fig 3H-I**). Serum levels of TaMCA, TbMCA and TCA were comparable in untreated, and vancomycin treated EAE mice (**Fig 3G**). We found that mice treated with vancomycin or ampicillin had very low serum level of all secondary bile acids (**Fig 3G-I**). We observed a slight increase in serum level of TUDCA in vancomycin treated naïve mice compared to untreated naïve mice (**Fig 3G**). However, serum TUDCA levels were higher in untreated EAE mice compared to untreated naïve mice as well as vancomycin and ampicillin treated EAE mice (**Fig 3G-H**). Furthermore, vancomycin treatment increased serum level of TUDCA in naïve mice but had no effect on TUDCA levels in EAE mice (**Fig 3G-H**). Taken together, our results suggest that elevated serum TUDCA could play a role in disease recovery in untreated EAE mice but not in vancomycin treated EAE mice. We found that untreated EAE mice had increased serum level of DCA compared to untreated naïve mice (**Fig 3G-H**). Vancomycin and ampicillin treated mice had negligible serum level of DCA (**Fig 3G-I**). Interestingly, prior studies have reported that DCA is pro-inflammatory in a mouse model of colitis[35–37]. Hence, our results suggest that depletion of DCA producing bacteria could be another mechanism accounting for vancomycin neuroprotective effect during the recovery phase of EAE.

Correlation between metabolites and bacteria abundance during the late stage of EAE

Indole derivatives, P-cresol and 4-EPS are gut commensals derived products. We found that vancomycin modulates the gut microbiota composition as well as serum levels of indole derivatives, p-cresol and 4-EPS in EAE mice. To assess if vancomycin induced changes in the gut microbiota

composition of EAE mice are linked to serum levels of tryptophan and tyrosine metabolites, we performed Spearman correlation between serum levels of these metabolites and bacterial abundance. We observed that 3-IS and P-cresol positively correlated with two taxa within the *Lachnospiraceae NK4A136* genus (ASV 81, ASV211), *Bacteroides* (ASV246) and four *Muribaculaceae* genera (ASV348, ASV363, ASV428 and ASV 487) (**Fig 4A-C; Fig S2**). Interestingly, these seven taxa were decreased in vancomycin treated EAE mice compared to untreated EAE mice (**Fig 2D-E**). We found that 3-IS and P-cresol were negatively correlated with a taxa within the *Enterobacteriaceae* genus (ASV284) (**Fig 4A-C**). In addition, *Enterobacteriaceae* genus (ASV284) was enriched in vancomycin treated EAE (**Fig 2D-E**). ILA and 4-EPS positively correlated with 4 *Clostridia vadinBB60 group* genera (ASV 124, ASV178, ASV434 and ASV449) and *Akkermansia municiphila* (ASV 231) (**Fig4A, 4D-E; Fig S2**). These five taxa were increased in vancomycin treated EAE mice compared to untreated EAE mice (**Fig 2D-E**). We observed that ILA negatively correlated with four *Muribaculaceae* genera (ASV348, ASV363, ASV428 and ASV 487) (**Fig 4A, 4D; Fig S2)** that were depleted in vancomycin treated EAE mice (**Fig 2D-E**) and positively correlated with 3-IS and p-cresol (**Fig 4B-C; Fig S2**). Consistent with the finding that 3-IS and p-cresol are neurotoxic[29], we observed that vancomycin treatment depleted bacteria linked with increased serum level of P-cresol and 3-IS and promoted the proliferation of bacteria linked with decreased serum levels of these metabolites. Consistent with prior studies reporting that ILA has anti-inflammatory properties and ameliorates EAE[27,28], we observed that vancomycin treatment promoted the proliferation of bacteria linked with increased serum level of 3-ILA.

As mentioned above, vancomycin treated mice had very low serum levels of bile acids compared to untreated mice. Given that secondary bile acids originate from the gut microbiota, we next run a Spearman correlation to examine if vancomycin induced changes in the gut microbiota composition of EAE mice are linked to serum levels of bile acids. We observed that serum levels of TUDCA and DCA (two secondary bile acids that have been implicated in autoimmune diseases) positively correlate with five taxa belonging to the *Muribaculaceae* genus (ASV179, ASV348, ASV363, ASV428 and ASV487), three taxa belonging to the *Lachnospiraceae NK4A136 group* genus (ASV005, ASV81, ASV211) and one taxa belonging to *Bacteroides* (ASV246) (**Fig 4A, 4F-G; Fig S2**). Interestingly, these taxa also positively correlate with serum P-cresol and/or 3-IS levels (**Fig 4B-C; Fig S2**) and were enriched in untreated EAE mice but depleted in vancomycin treated EAE mice (**Fig 2D-E**). Consistent with prior studies showing that DCA is a pro-inflammatory bile acid[35–37], we found that vancomycin treatment depleted bacteria linked with increased serum level of DCA.

Astrocytes from vancomycin treated mice exhibit distinct transcriptomes during late stage of EAE

Since $CD4^+$ T cells are key players in the pathogenesis of the EAE model we tested the effects of vancomycin and ampicillin on $CD4^+$ T cell cytokine production and noted no direct anti-inflammatory effects of vancomycin and ampicillin on $CD4^+$ T cells (**Fig S3**). These findings suggest that vancomycin and ampicillin do not appear to mediate their effects on EAE through alteration of T cell function.

Prior studies have reported that astrocytes derived pathways are important modulator of neuroinflammation during the recovery phase of EAE[15]. Furthermore, indole derivatives and secondary bile acid, TUDCA, have been shown to modulate astrocyte function during the recovery phase of EAE[15,34]. We observed that vancomycin treatment initiated in the early stage of EAE (prior to symptoms onset) improved disease recovery and altered serum levels of indole derivatives and secondary bile acids. Hence, to assess how vancomycin induced changes in serum levels of indoles and secondary bile acids affect astrocyte function, we performed RNA sequencing (RNA Seq). Bulk RNA sequencing detected 17690 genes of which 3422 were differentially expressed (**Fig S4-5A**).

We found that vancomycin treatment altered the expression of 1414 genes in astrocytes from EAE mice compared to untreated EAE mice. 1030 genes were differentially in astrocytes from vancomycin treated EAE mice versus ampicillin treated EAE mice. Astrocyte isolated from vancomycin treated EAE mice showed decreased levels of pro-inflammatory genes including Tspo (**Fig 5A, 5G**) as well as increased expression of genes with antimicrobial activity like Ccl12 and Cxcl14 (**Fig 5A, 5G**). A study showed that indole derivatives: 3-IS, 3-IPA and indole-3-aldehyde, binding to Ahr on astrocytes

induces anti-inflammatory pathways suppressing neuroinflammation during the recovery phase of EAE[15]. We observed increased Ahr expression in astrocytes from ampicillin treated EAE mice (**Fig 5B-C, 5G**). Furthermore, ampicillin treated EAE mice had good 3-ILA serum level whereas serum levels of 3-IS and 3-IPA were negligible (**Fig 3A-C**). Vancomycin treatment did not change Ahr expression on astrocytes (**Fig 5A-C, 5G**) but we observed increased serum level of indole-3-lactic acid in vancomycin treated EAE mice compared to untreated and ampicillin treated EAE mice (**Fig 3B-C**). Taken together, our results suggest that the neuroprotective effects of vancomycin and ampicillin treatments may be in part mediated via activation of Ahr on astrocytes by 3-ILA.

Another group of genes in astrocytes whose expression was modulated by vancomycin belong to the mTOR pathway. We found that vancomycin treatment induced increased expression of Hk2, Fdxr, Nufip1, Acsl3 in astrocytes of EAE mice compared to untreated EAE mice (**Fig 5D-F, 5H**). We observed that vancomycin treatment induced downregulation of Dhfr, Tomm40, Stard4, Asns, Gla, Pik3r3, Nfil3 and Gmps compared to untreated EAE mice (**Fig 5D-F, 5H**).

Correlation between mTOR genes, bacteria abundance and metabolites during late stage of EAE

Prior studies have shown that indole derivatives and secondary bile acid, TUDCA, modulate astrocyte function during the recovery phase of EAE. Furthermore, we found that vancomycin treatment modulates gut microbiota composition, serum levels of indole derivatives, p-cresol, 4-EPS and secondary bile acids. We also observed that vancomycin induced changes in the expression of many genes in astrocytes including those belonging to the mTOR pathway. To determine if there is a link between level of expression of mTOR pathway genes in astrocytes, gut commensals abundance and serum levels of indole derivatives, p-cresol, 4-EPS and secondary bile acids, we performed Spearman correlation. Fdxr positively correlated with *Enterobacteriaceae* genus (ASV284) and negatively correlated with 3-IS, P-cresol, DCA, LCA and TDCA (**Fig. 6A-B**). Nufip1 negatively correlated with *Turicibacter* genus (ASV438), 3-IS, P-cresol and TDCA. Ascl3 negatively correlated with 2 *Lachnospiraceae NK4A136 group* genera (ASV005, ASV 211), P-cresol, DCA, LCA, GLCA, TDCA, TLCA (**Fig. 6A-B)**. Fdxr, Nufip and Ascl3 were upregulated in vancomycin treated EAE mice compared to untreated EAE mice (**Fig 5A, 5H**). Genes upregulated in astrocytes from vancomycin treated EAE mice are linked with decreased serum levels of 3-IS, p-cresol, DCA and TDCA (**Fig 6B**).

Dhfr negatively correlated with 6 *Clostridia vadinBB60 group* genera (ASV54, ASV124, ASV178, ASV182, ASV434, ASV449), 3-ILA and 4-EPS (**Fig. 6A-B**). Tomm40 positively correlated with *Lachnospiraceae NK4A136 group* genus (ASV81), ASV246, 3 *Muribaculaceae* genera (ASV363, ASV428, ASV487), DCA, LCA, TDCA, TLCA and negatively correlated with 2 *Clostridia vadinBB60 group* genera (ASV124, ASV449), *Akkermansia municiphila* (ASV231), 3-ILA and 4-EPS (**Fig. 6A-B**). Nfil3 positively correlated with *Lachnospiraceae NK4A136 group* genus (ASV81), *Bacteroides* genus (ASV246), *Muribaculaceae* genus (ASV428), DCA, LCA, GLCA, TDCA, TLCA and p-cresol (**Fig. 6A-B**). Gmps positively correlated with *Bacteroides* genus (ASV246), 3 *Muribaculaceae* genera (ASV363, ASV 428, ASV 487) and negatively correlated with 4 *Clostridia vadinBB60 group* genera (ASV124, ASV178, ASV434, ASV449), 3-ILA and 4-EPS (**Fig. 6A-B**). Dhfr, Tomm40, Nfil3 and Gmps were downregulated in vancomycin treated EAE mice compared to untreated EAE mice (**Fig 5D-F, 5H**). Genes downregulated in astrocytes from vancomycin treated EAE mice are linked with either increased serum level of 3-ILA and 4-EPS or decreased serum levels of P-cresol, DCA and TDCA.

Lactobacillus reuteri modulate mTOR pathway genes expression in astrocytes during late stage of EAE

Our correlation studies suggest that vancomycin modulate the expression of genes belonging to the mTOR pathway at least in part by promoting the proliferation of ILA-producing bacteria. Several *Lactobacillus* species are known indole producers and given that we have previously observed increased abundance of *Lactobacillus* species in vancomycin treated mice, we examine the relative abundance of Lactobacilli in our mice. We observed increased relative abundance of 4 *Lactobacillus* species in vancomycin and ampicillin treated naïve mice (**Fig 7A**). We have previously observed

increased abundance of *L. reuteri*, a ILA-producing gut commensal, in vancomycin treated EAE mice[14]. Consistent with these findings, we found that *L. reuteri* was increased in vancomycin and ampicillin treated mice compared to untreated mice (**Fig 7A**). Of note, *L. reuteri* was below the level of detection in EAE mice but this does not mean that it was not present (**Fig 7A).** Hence, it is conceivable that *L. reuteri* was one the ILA-producing bacteria in EAE mice treated with vancomycin and ampicillin.
Prior studies have reported that *L. reuteri* ameliorates EAE[38,39] and three other studies reported that *L. reuteri* exacerbates EAE[33,40,41]. Hence, to determine how *L. reuteri* affect EAE development in our environment, B6 mice were gavage with *L. reuteri* pre- EAE induction (green group) or at day 16 post immunization (black group). We found that administration of *L. reuteri* ameliorates disease recovery (**Fig 7B**).

Given that we observed a correlation between ILA levels and the expression of several genes belonging to the mTOR pathway, we next performed bulk RNA sequencing to examine the effect of *L. reuteri* on mTOR gene pathway expression in astrocytes. Bulk RNA seq revealed 22128 expressed genes of which 1118 were differentially expressed between *L. reuteri* and vehicle (**P<0.05; Fig S4-5B**). We found that *L. reuteri* regulate the expression of 10 genes belonging to the mTOR pathway in astrocytes (**Fig 7C**). We observed increased expression of Acsl3 and Slc1a4 in astrocytes from *L. reuteri* treated mice compared to mice who received vehicle (**Fig 7C**). Interestingly, Acsl3 expression was increased in vancomycin and ampicillin treated EAE mice compared to untreated EAE mice (**Fig 5D-E**). Slc1a4 expression was increased in ampicillin treated mice (**Fig 5E**). Ascl3 expression in vancomycin treated negatively correlated with serum level of DCA. Interestingly, we observed decreased serum DCA level in *L. reuteri* fed mice compared to mice receiving vehicle (data not shown). Taken together, these results suggest that increased ILA:DCA ratio in vancomycin treated mice and *L. reuteri* fed mice leads to increased Acsl3 expression.

DISCUSSION

Over the past several years, many pre-clinical and clinical studies have gathered findings supporting a role of the gut microbiota in the pathophysiology of MS. Notably, a prior study showed that binding of gut commensals derived tryptophan metabolites, indole derivatives, on the Ahr receptor in astrocytes triggered pathways that suppress neuroinflammation during the late stage of EAE[15]. These findings suggest that indole-producing bacteria modulate astrocyte function however, the identity of these bacteria remains obscure. Here we show that oral administration of vancomycin to EAE mice during the early stage of EAE (prior to symptoms onset) ameliorate disease recovery. We observed an increase in the abundance of gut commensals belonging to the genus *Clostridia vadinBB60 group* in vancomycin treated EAE mice compared to untreated EAE mice. Interestingly, one study reported decreased abundance of *Clostridia vadinBB60 group* in treatment naïve MS patients compared to treated MS patients or healthy subjects[26]. Another study reported depletion of *Clostridia vadinBB60 group* in EAE mice compared to naïve mice starting at 8 days post immunization[39]. These findings suggest that *Clostridia vadinBB60 group* may have anti-inflammatory properties. Consistent with this notion, two studies have reported that *Clostridia vadinBB60 group* is protective in IBD[42,43].

Given prior reports that indoles derivatives and the secondary bile acid, TUDCA, modulate astrocyte function during the chronic phase of EAE, we next examine the effect of vancomycin on serum levels of these metabolites. We found increased serum levels of ILA and decreased IPA, 3-IS and p-cresol in vancomycin treated EAE mice compared to untreated EAE mice. Interestingly, ILA has been shown to have anti-inflammatory properties. Furthermore, another study reported that ILA is decreased in progressive MS patients compared to relapsing-remitting MS (RRMS) patients[30]. Consistent with these findings, another group identified ILA as one of the most depleted serum metabolites in MS compared to controls[44]. Interestingly, we found a positive correlation between serum level of ILA and abundance of several taxa belonging to genus *Clostridia vadinBB60 group*. Hence, these data suggest that *Clostridia vadinBB60 group* may produce ILA and this could account for its anti-inflammatory effect. Future studies in gnotobiotic mice are warranted to characterize the interaction between taxa belonging to genus *Clostridia vadinBB60 group* and the host during EAE. One study reported that 3-IPA and 3-IS ameliorate disease during the chronic phase of EAE[15]. However, another study showed that several

tryptophan metabolites are pro-inflammatory and exacerbate EAE[33]. Furthermore, another study showed that 3-IS and p-cresol are neurotoxins[29]. Consistent with these findings, another study reported increased level of p-cresol in progressive MS patients compared to RRMS[30]. We observed decreased serum levels of DCA in vancomycin treated EAE mice compared to untreated EAE mice. DCA level has not been studied in EAE mice. Studies have reported that DCA exacerbates inflammation in a mouse model of colitis[35–37]. Hence, these results suggest that vancomycin treatment improve disease recovery by eliminating neurotoxins (3-IS and p-cresol) producing or pro-inflammatory metabolites (DCA) producing gut commensals and triggering proliferation of bacteria producing anti-inflammatory metabolites (ILA). Of note, we found that serum bile acids levels were increased in untreated EAE mice compare to untreated naïve mice. Notably, we observed increased serum TUDCA in untreated EAE mice compared to naïve untreated mice. Given prior report that TUDCA ameliorates disease recovery in EAE mice[34], elevated TUDCA level in untreated EAE mice could be a host response to suppress neuroinflammation thus allowing mice to enter the recovery phase of the disease. Of note, even though vancomycin increased serum level of TUDCA in naïve mice, it had no effect on TUDCA level in EAE mice.

Given prior reports that indole derivatives and TUDCA modulate astrocyte function[15,34], we next examine the effect of vancomycin on astrocytes transcriptional profile. We found that vancomycin treatment modulates the expression of several genes belonging to the mTOR pathway. Interestingly, prior studies have shown that inhibiting the mTOR pathway ameliorates EAE via inducing T regulatory cells or suppressing Th1 and/or Th17 cells[45,46]. However, to date, no study has examined the role of the mTOR pathway in astrocytes during EAE. We observed upregulation of Fdxr, Acsl3 and Nufip1 genes belonging to the mTOR pathway in vancomycin treated EAE mice compared to untreated EAE mice. Interestingly, one study reports that naturally-occuring mouse model with homozygous Fdxr mutations displayed optic atrophy as well as atrophy of the cerebellum and cerebral cortex[47]. They also observed increase in markers of both neurodegeneration and glial activation in these Fdxr mutant mice[47]. These findings suggest that loss of function of Fdxr leads to neuronal loss. Hence, the increased in Fdxr expression that we observed in our vancomycin treated EAE mice compared to untreated EAE mice could have neuroprotective effects. Future studies using astrocyte specific Fdxr KO mice are needed to elucidate the function of this gene during EAE. The functions of Acsl3 and Nufip1 in astrocytes remain unknown. Interestingly, we found that mTOR pathway genes that are upregulated in astrocytes from vancomycin treated mice had a positive correlation with a taxa enriched in vancomycin treated EAE mice, *Enterobacteriaceae* genus (ASV284), and a negative correlation with taxa enriched in untreated EAE mice namely *Muribaculaceae* and *Lachnospiraceae NK4A136 group* genera. We also observed that mTOR pathway genes that are upregulated in astrocytes from vancomycin treated mice negatively correlate with serum levels of p-cresol, 3-IS and DCA. mTOR pathway genes that were downregulated in astrocytes from vancomycin treated EAE mice had a negative correlation with taxa enriched in vancomycin treated mice, vadinBB60 group genus, and/or a positive correlation with taxa enriched in untreated EAE mice, *Muribaculaceae* and *Lachnospiraceae NK4A136 group* genera.

mTOR genes that are downregulated in astrocytes from vancomycin treated mice negatively correlate with serum level of ILA (metabolite enriched in vancomycin treated mice) but positively correlate with serum levels of 3-IS, p-cresol and DCA (metabolites enriched in untreated EAE mice). Interestingly, *Lactobacilli reuteri*, an ILA producing bacteria, was enriched in vancomycin treated mice. We found that EAE mice fed *L. reuteri* had improved disease recovery compared to mice receiving vehicle. Consistent with this finding, prior studies have reported that *L. reuteri* ameliorates EAE[38,39]. In addition, mice that received *L. reuteri* had altered gene expression of mTOR pathway genes in astrocytes notably a gene upregulated in vancomycin treated EAE mice, Ascl3, was also upregulated in *L. reuteri* fed mice. Ascl3 expression was associated with decreased DCA serum level in *L. reuteri* fed mice as well as vancomycin treated EAE mice. Hence, it could be that high ILA level leads to decreased DCA levels which then leads to increased Ascl3 expression. Consistent with this notion, one study reported that high level of anti-inflammatory metabolite, butyrate, is associated with low level of DCA[48]. Hence, these results suggest that indoles derivatives and DCA can modulate the expression of mTOR pathway genes in astrocytes (**Fig 8:** hypothesized model diagram). Consistent with this notion,

studies have reported that indole derivatives as well as secondary bile acids regulate the mTOR pathway[49–52]. Furthermore, another study reported that *L. reuteri* modulates mTOR expression[53]. mTOR pathway has been implicated in several inflammatory and neurodegenerative diseases including MS[45,54–57]. Hence, more studies are needed to elucidate the mechanisms by which indoles derivatives and DCA modulate the expression of mTOR pathway genes in astrocytes during EAE.

Our results also revealed that some indole derivatives as well as secondary bile acids are pro-inflammatory/neurotoxic while other are anti-inflammatory/neuroprotective. Furthermore, even though we and other groups have found 3-IS to be neurotoxic in EAE mice and MS patients respectively, another study reported that this indole derivative is neuroprotective in EAE mice. These results suggest that the host clinical phenotype may be determined by several factors including the ratio of pro- to anti-inflammatory metabolites as well as the microbiome composition and host genetics. This could also explain discrepancies between studies examining the effect of a bacteria in the host. For example, contrary to our findings, some studies have observed that *L. reuteri* exacerbates EAE. This apparent discrepancy could be explained by differences in ratios of neurotoxic to neuroprotective metabolites as well as differences in microbiome composition in each experimental setting.

Our study has some limitations. Although we observed increased abundance of the *Clostridia vadinBB60 group* in vancomycin-treated EAE mice and a correlation between this taxa and expression of mTOR pathway genes in astrocytes, we cannot establish a causal effect. Additional studies will be required to determine whether colonization with this taxa alone is sufficient to modulate expression of genes in the mTOR pathway. Furthermore, we observed that vancomycin altered the expression of several genes in the mTOR pathway in astrocytes but their functions during neuroinflammation remain unknown. Our work adds to the growing literature on the importance of the mTOR pathway role in CNS inflammatory and neurodegenerative diseases. Previous studies have shown that rapamycin, a specific inhibitor of mTOR, ameliorates EAE via suppression of T effector cells or inducing T regulatory cells[45]. To this date, there are no published studies examining the role of the mTOR pathway in astrocytes during EAE. Hence future studies using astrocytes specific KO of mTOR pathway genes of interest are warranted to elucidate the mechanism by which vancomycin induced changes in astrocytes transcriptional profile regulate neuroinflammation during EAE. Finally, our findings suggest that indoles derivatives as well as bile acids modulate mTOR pathway genes expression in astrocytes during EAE. Future studies using Ahr and G-protein coupled bile acid receptor astrocytes specific KO should be conducted to investigate the effect of indole derivatives and bile acids on the expression of mTOR pathway genes.

Despite these limitations, our study showed that vancomycin modulates astrocyte function during the chronic phase of EAE. We also observed that vancomycin induced the production of indole-3-lactic acid, an anti-inflammatory metabolite, that is decreased in progressive MS compared to relapsing-remitting MS patients. Furthermore, another group reports that in addition to inhibiting neuroinflammation in MOG induced EAE mice, ILA also promotes remyelination in the cuprizone EAE mouse model (Larissa Jank et al; ACTRIMS 2024 abstract)[58]. These findings suggest that vancomycin could be beneficial for progressive MS patients. While we are currently running a double-blind, placebo-controlled randomized trial to investigate the clinical impact of vancomycin in newly diagnosed, treatment naive MS patients (NCT05539729), future trials will be required to examine the effect of vancomycin in progressive MS patients with low level of ILA.

ABBREVIATIONS

3-ILA: 3 Indole Lactic Acid

3-IPA: 3-Indole Propionic Acid

3-IS: 3-Indoxyl Sulphate

4-EPS: 4-Ethyl Phenyl Sulphate

AhR: Aryl Hydrocarbon receptor

aMCA: Alpha Muricholic Acid

bMCA: Beta Muricholic Acid

CA: Cholic Acid

CDCA: Chenodeoxycholic Acid

CNS: Central Nervous System

DCA: Deoxycholic Acid

EAE: Experimental Autoimmune Encephalomyelitis

GCA: Glycocholic Acid

GCDCA: Glycochenodeoxycholic Acid

GDCA: Glycodeoxycholic Acid

GLCA: Glycolithocholic Acid

GUDCA: Glycoursodeoxycholic Acid

IBD: Inflammatory Bowel Disease

LCA: Lithocholic Acid

MS: Multiple Sclerosis

mTOR: mammalian Target Of Rapamycin

oMCA: Omega Muricholic Acid

p-Cresol: p-Cresol Sulphate

RNA Seq: RNA Sequencing

TaMCA: Tauro Alpha Muricholic Acid

TbMCA: Tauro Beta Muricholic Acid

TCA: Taurocholic Acid

TCDCA: Taurochenodeoxycholic Acid

TDCA: Taurodeoxycholic Acid

TLCA: Taurolithocholic Acid

Trp: Tryptophan

TUDCA: Tauroursodeoxycholic Acid

UDCA: Ursodeoxycholic Acid

AUTHORS' CONTRIBUTION

SKT, PB, PL, CGV and EMS performed experiments; EW, PB, GB and JCC analyzed the microbiome data; PB analyzed the RNA-Seq data; SKT, PB and PL generated the figures; and SKT and PB wrote the manuscript with input from all authors. SKT conceived the study, designed the analysis, and finalized the manuscript. The authors read and approved the final manuscript.

DECLARATION OF COMPETING INTEREST

The authors declare that they have no known competing financial interests or personal relationships that could have appeared to influence the work reported in this paper.

DATA AVAILABILITY

The microbiota 16S rRNA sequence data as well as RNA sequencing data will be submitted to the Mendeley Data Repository and made available to the public once the paper is published.

ACKNOWLEDGMENTS

We acknowledge the support of the Dean's Flow Cytometry CORE at the Icahn School of Medicine at Mount Sinai. We would like to thank Dr. Francisco Quintana for providing us with a detailed protocol for isolation of astrocytes from mouse spinal cords.

FUNDING

This work was supported by the Department of Neurology, Icahn School of Medicine at Mount Sinai and the National MS Society.

REFERENCES

1. Lassmann, H. Pathogenic Mechanisms Associated With Different Clinical Courses of Multiple Sclerosis. *Front. Immunol.* **9**, 3116 (2019).
2. Frischer, J. M. *et al.* Clinical and pathological insights into the dynamic nature of the white matter multiple sclerosis plaque. *Ann. Neurol.* **78**, 710–721 (2015).
3. Allen, N. J. *et al.* Astrocyte glypicans 4 and 6 promote formation of excitatory synapses via GluA1 AMPA receptors. *Nature* **486**, 410–414 (2012).
4. Khakh, B. S. & Sofroniew, M. V. Diversity of astrocyte functions and phenotypes in neural circuits. *Nat. Neurosci.* **18**, 942–952 (2015).
5. Obermeier, B., Daneman, R. & Ransohoff, R. M. Development, maintenance and disruption of the blood-brain barrier. *Nat. Med.* **19**, 1584–1596 (2013).
6. Sofroniew, M. V. Astrocyte barriers to neurotoxic inflammation. *Nat Rev Neurosci* **16**, 249–263 (2015).
7. Absinta, M. *et al.* A lymphocyte–microglia–astrocyte axis in chronic active multiple sclerosis. *Nature* **597**, 709–714 (2021).
8. Yi, W., Schlüter, D. & Wang, X. Astrocytes in Multiple Sclerosis and Experimental Autoimmune Encephalomyelitis: star-shaped cells illuminating the darkness of CNS autoimmunity. *Brain Behav Immun* **80**, 10–24 (2019).
9. Lassmann, H. Mechanisms of white matter damage in multiple sclerosis. *Glia* **62**, 1816–1830 (2014).
10. Shao, W. *et al.* Suppression of neuroinflammation by astrocytic dopamine D2 receptors via αB-crystallin. *Nature* **494**, 90–94 (2013).
11. Consortium, iMSMS *et al.* Gut microbiome of multiple sclerosis patients and paired household healthy controls reveal associations with disease risk and course. *Cell* **185**, 3467-3486.e16 (2022).
12. Cox, L. M. *et al.* Gut Microbiome in Progressive Multiple Sclerosis. *Ann Neurol* **89**, 1195–1211 (2021).
13. Bianchimano, P. *et al.* Mining the microbiota to identify gut commensals modulating neuroinflammation in a mouse model of multiple sclerosis. *Microbiome* **10**, 174 (2022).
14. Bianchimano, P. *et al.* Oral vancomycin treatment suppresses gut trypsin activity and preserves intestinal barrier function during EAE. *iScience* **26**, 108143 (2023).
15. Rothhammer, V. *et al.* Type I interferons and microbial metabolites of tryptophan modulate astrocyte activity and central nervous system inflammation via the aryl hydrocarbon receptor. *Nat Med* **22**, 586–597 (2016).

16. Kozich, J. J., Westcott, S. L., Baxter, N. T., Highlander, S. K. & Schloss, P. D. Development of a Dual-Index Sequencing Strategy and Curation Pipeline for Analyzing Amplicon Sequence Data on the MiSeq Illumina Sequencing Platform. *Appl Environ Microb* **79**, 5112–5120 (2013).
17. Bokulich, N. A. *et al.* Optimizing taxonomic classification of marker-gene amplicon sequences with QIIME 2's q2-feature-classifier plugin. *Microbiome* **6**, 90 (2018).
18. Trombetta, J. J. *et al.* Preparation of Single-Cell RNA-Seq Libraries for Next Generation Sequencing. *Curr. Protoc. Mol. Biol.* **107**, 4.22.1-4.22.17 (2014).
19. Bolger, A. M., Lohse, M. & Usadel, B. Trimmomatic: a flexible trimmer for Illumina sequence data. *Bioinformatics* **30**, 2114–2120 (2014).
20. Dobin, A. *et al.* STAR: ultrafast universal RNA-seq aligner. *Bioinformatics* **29**, 15–21 (2012).
21. Li, B. & Dewey, C. N. RSEM: accurate transcript quantification from RNA-Seq data with or without a reference genome. *BMC Bioinform.* **12**, 323 (2011).
22. Love, M. I., Huber, W. & Anders, S. Moderated estimation of fold change and dispersion for RNA-seq data with DESeq2. *Genome Biol* **15**, 550 (2014).
23. Schmittgen, T. D. & Livak, K. J. Analyzing real-time PCR data by the comparative CT method. *Nat Protoc* **3**, 1101–1108 (2008).
24. Zhang, M., Zhang, M., Kou, G. & Li, Y. The relationship between gut microbiota and inflammatory response, learning and memory in mice by sleep deprivation. *Front. Cell. Infect. Microbiol.* **13**, 1159771 (2023).
25. Liu, S. *et al.* Oral Administration of miR-30d from Feces of MS Patients Suppresses MS-like Symptoms in Mice by Expanding Akkermansia muciniphila. *Cell Host Microbe* (2019) doi:10.1016/j.chom.2019.10.008.
26. Tremlett, H. *et al.* The gut microbiota in pediatric multiple sclerosis and demyelinating syndromes. *Ann. Clin. Transl. Neurol.* **8**, 2252–2269 (2021).
27. Wilck, N. *et al.* Salt-responsive gut commensal modulates TH17 axis and disease. *Nature* **551**, 585 (2017).
28. Alexander, M. *et al.* A diet-dependent host metabolite shapes the gut microbiota to protect from autoimmunity. *bioRxiv* 2023.11.02.565382 (2024) doi:10.1101/2023.11.02.565382.
29. Ntranos, A. *et al.* Bacterial neurotoxic metabolites in multiple sclerosis cerebrospinal fluid and plasma. *Brain* (2021) doi:10.1093/brain/awab320.
30. Fitzgerald, K. C. *et al.* Multi-omic evaluation of metabolic alterations in multiple sclerosis identifies shifts in aromatic amino acid metabolism. *Cell Rep. Med.* **2**, 100424 (2021).
31. Needham, B. D. *et al.* A gut-derived metabolite alters brain activity and anxiety behaviour in mice. *Nature* **602**, 647–653 (2022).
32. Gacias, M. *et al.* Microbiota-driven transcriptional changes in prefrontal cortex override genetic differences in social behavior. *Elife* **5**, e13442 (2016).
33. Montgomery, T. L. *et al.* Lactobacillus reuteri tryptophan metabolism promotes host susceptibility to CNS autoimmunity. *Microbiome* **10**, 198 (2022).
34. Bhargava, P. *et al.* Bile acid metabolism is altered in multiple sclerosis and supplementation ameliorates neuroinflammation. *J Clin Investigation* (2020) doi:10.1172/jci129401.
35. Ju, J. *et al.* Deoxycholic acid exacerbates intestinal inflammation by modulating interleukin-1β expression and tuft cell proportion in dextran sulfate sodium-induced murine colitis. *PeerJ* **11**, e14842 (2023).
36. Li, D. *et al.* Gut microbial metabolite deoxycholic acid facilitates Th17 differentiation through modulating cholesterol biosynthesis and participates in high-fat diet-associated colonic inflammation. *Cell Biosci.* **13**, 186 (2023).
37. Zhao, S. *et al.* Deoxycholic Acid Triggers NLRP3 Inflammasome Activation and Aggravates DSS-Induced Colitis in Mice. *Front. Immunol.* **7**, 536 (2016).
38. He, B. *et al.* Lactobacillus reuteri Reduces the Severity of Experimental Autoimmune Encephalomyelitis in Mice by Modulating Gut Microbiota. *Front Immunol* **10**, 385 (2019).
39. Johanson, D. M. *et al.* Experimental autoimmune encephalomyelitis is associated with changes of the microbiota composition in the gastrointestinal tract. *Sci Rep-uk* **10**, 15183 (2020).

40. Miyauchi, E. *et al.* Gut microorganisms act together to exacerbate inflammation in spinal cords. *Nature* **585**, 102–106 (2020).
41. Montgomery, T. L. *et al.* Interactions between host genetics and gut microbiota determine susceptibility to CNS autoimmunity. *Proc National Acad Sci* **117**, 27516–27527 (2020).
42. Liu, J. *et al.* Alanyl-Glutamine (Ala-Gln) Ameliorates Dextran Sulfate Sodium (DSS)-Induced Acute Colitis by Regulating the Gut Microbiota, PI3K-Akt/NF-κB/STAT3 Signaling, and Associated Pulmonary Injury. *ACS Infect. Dis.* **9**, 979–992 (2023).
43. Li, F. *et al.* Mendelian randomization distinguished the changes in gut microbiota caused by IBD from those that lead to IBD. (2024) doi:10.21203/rs.3.rs-3897238/v1.
44. Levi, I. *et al.* Potential role of indolelactate and butyrate in multiple sclerosis revealed by integrated microbiome-metabolome analysis. *Cell Rep. Med.* **2**, 100246 (2021).
45. Vakrakou, A. G. *et al.* The mTOR Signaling Pathway in Multiple Sclerosis; from Animal Models to Human Data. *Int. J. Mol. Sci.* **23**, 8077 (2022).
46. Hou, H. *et al.* Rapamycin and fingolimod modulate Treg/Th17 cells in experimental autoimmune encephalomyelitis by regulating the Akt-mTOR and MAPK/ERK pathways. *J. Neuroimmunol.* **324**, 26–34 (2018).
47. Slone, J. *et al.* Biallelic mutations in FDXR cause neurodegeneration associated with inflammation. *J. Hum. Genet.* **63**, 1211–1222 (2018).
48. Niekamp, P. & Kim, C. H. Microbial Metabolite Dysbiosis and Colorectal Cancer. *Gut Liver* **17**, 190–203 (2023).
49. Chao, S. *et al.* Lithocholic acid activates mTOR signaling inducing endoplasmic reticulum stress in placenta during intrahepatic cholestasis of pregnancy. *Life Sci.* **218**, 300–307 (2019).
50. Huang, R., Huang, Y., Zeng, G., Li, M. & Jin, Y. Ursodeoxycholic acid inhibits intimal hyperplasia, vascular smooth muscle cell excessive proliferation, migration via blocking miR-21/PTEN/AKT/mTOR signaling pathway. *Cell Cycle* **19**, 918–932 (2020).
51. Ahmad, A. *et al.* Targeted Regulation of PI3K/Akt/mTOR/NF-κB Signaling by Indole Compounds and their Derivatives: Mechanistic Details and Biological Implications for Cancer Therapy. *Anti-Cancer Agents Med. Chem.* **13**, 1002–1013 (2013).
52. Nicastro, R. *et al.* Indole-3-acetic acid is a physiological inhibitor of TORC1 in yeast. *PLoS Genet.* **17**, e1009414 (2021).
53. Cui, Y. *et al.* Lactobacillus reuteri ZJ617 maintains intestinal integrity via regulating tight junction, autophagy and apoptosis in mice challenged with lipopolysaccharide. *Oncotarget* **5**, 77489–77499 (2014).
54. Switon, K., Kotulska, K., Janusz-Kaminska, A., Zmorzynska, J. & Jaworski, J. Molecular neurobiology of mTOR. *Neuroscience* **341**, 112–153 (2017).
55. Li, C.-Y. *et al.* Inhibition of mTOR pathway restrains astrocyte proliferation, migration and production of inflammatory mediators after oxygen–glucose deprivation and reoxygenation. *Neurochem. Int.* **83**, 9–18 (2015).
56. Wang, X., Sha, L., Sun, N., Shen, Y. & Xu, Q. Deletion of mTOR in Reactive Astrocytes Suppresses Chronic Seizures in a Mouse Model of Temporal Lobe Epilepsy. *Mol. Neurobiol.* **54**, 175–187 (2017).
57. Ceccariglia, S., Sibilia, D., Parolini, O., Michetti, F. & Sante, G. D. Altered Expression of Autophagy Biomarkers in Hippocampal Neurons in a Multiple Sclerosis Animal Model. *Int. J. Mol. Sci.* **24**, 13225 (2023).
58. ACTRIMS Forum 2024 - Abstract Sessions and Invited Sessions.

Figure 1

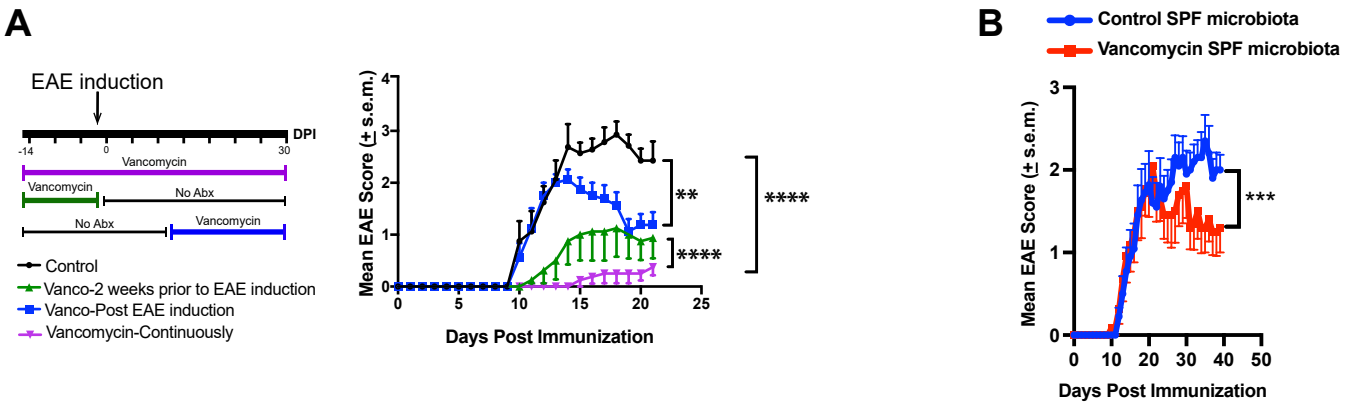
A
EAE induction
DPI
-14
0
30
Vancomycin
Vancomycin
No Abx
No Abx
Vancomycin
Control
Vanco-2 weeks prior to EAE induction
Vanco-Post EAE induction
Vancomycin-Continuously
Mean EAE Score (± s.e.m.)
Days Post Immunization
**
****
****
B
Control SPF microbiota
Vancomycin SPF microbiota
Mean EAE Score (± s.e.m.)
Days Post Immunization
***

Figure 1. Vancomycin effect on EAE development is mediated via the gut microbiota and is dependent on the length and timing of administration. Conventionally raised mice were either untreated or vancomycin treated via oral gavage either prior to or post immunization with MOG for EAE induction **(A)** Experimental timeline for vancomycin administration (left), and Mean EAE clinical scores over time (right) in untreated and vancomycin-treated mice. Error bars denote mean ± SEM (n = 8-10 mice/group). Representative data of three independent experiments. Data were analyzed using Freidman test with Dunn's correction for multiple comparisons. *p< 0.05, **p< 0.01, ***p< 0.001, ****p< 0.0001. Conventionally raised mice were immunized with MOG for EAE induction and starting at day 15 post immunization, half of the mice received microbiota from untreated mice and the remaining half received microbiota from vancomycin treated mice daily until the end of the experiment. **(B)** Mean EAE clinical scores overtime. Error bars denote mean ± SEM (n = 8-10 mice/group). Shown are representative data from two independent experiments. Freidman test with Dunn's correction for multiple comparisons. *p< 0.05, **p< 0.01, ***p< 0.001, ****p< 0.0001. SPF: specific pathogen free.

Figure 2

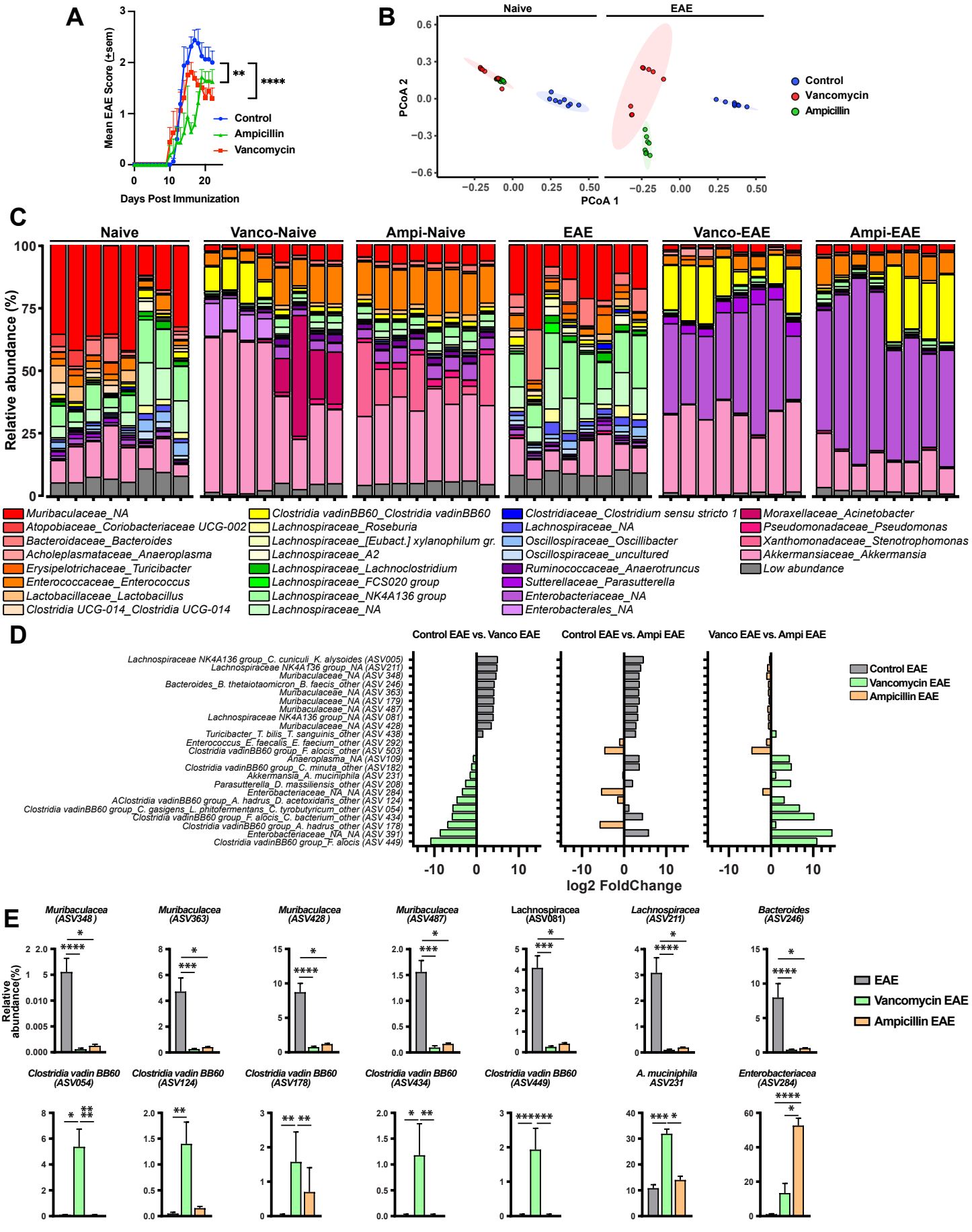
A
Mean EAE Score (±sem)
Days Post Immunization
Control
Ampicillin
Vancomycin
**
****
B
Naive
EAE
PCoA 2
PCoA 1
Control
Vancomycin
Ampicillin
C
Naive
Vanco-Naive
Ampi-Naive
EAE
Vanco-EAE
Ampi-EAE
Relative abundance (%)
Muribaculaceae_NA
Atopobiaceae_Coriobacteriaceae UCG-002
Bacteroidaceae_Bacteroides
Acholeplasmataceae_Anaeroplasma
Erysipelotrichaceae_Turicibacter
Enterococcaceae_Enterococcus
Lactobacillaceae_Lactobacillus
Clostridia UCG-014_Clostridia UCG-014
Clostridia vadinBB60_Clostridia vadinBB60
Lachnospiraceae_Roseburia
Lachnospiraceae_[Eubact.] xylanophilum gr.
Lachnospiraceae_A2
Lachnospiraceae_Lachnoclostridium
Lachnospiraceae_FCS020 group
Lachnospiraceae_NK4A136 group
Lachnospiraceae_NA
Clostridiaceae_Clostridium sensu stricto 1
Lachnospiraceae_NA
Oscillospiraceae_Oscillibacter
Oscillospiraceae_uncultured
Ruminococcaceae_Anaerotruncus
Sutterellaceae_Parasutterella
Enterobacteriaceae_NA
Enterobacterales_NA
Moraxellaceae_Acinetobacter
Pseudomonadaceae_Pseudomonas
Xanthomonadaceae_Stenotrophomonas
Akkermansiaceae_Akkermansia
Low abundance
D
Control EAE vs. Vanco EAE
Control EAE vs. Ampi EAE
Vanco EAE vs. Ampi EAE
Lachnospiraceae NK4A136 group_C. cuniculi_K. alysoides (ASV005)
Lachnospiraceae NK4A136 group_NA (ASV211)
Muribaculaceae_NA (ASV 348)
Bacteroides_B. thetaiotaomicron_B. faecis_other (ASV 246)
Muribaculaceae_NA (ASV 363)
Muribaculaceae_NA (ASV 179)
Muribaculaceae_NA (ASV 487)
Lachnospiraceae NK4A136 group_NA (ASV 081)
Muribaculaceae_NA (ASV 428)
Turicibacter_T. bilis_T. sanguinis_other (ASV 438)
Enterococcus_E. faecalis_E. faecium_other (ASV 292)
Clostridia vadinBB60 group_F. alocis_other (ASV 503)
Anaeroplasma_NA (ASV109)
Clostridia vadinBB60 group_C. minuta_other (ASV182)
Akkermansia_A. muciniphila (ASV 231)
Parasutterella_D. massiliensis_other (ASV 208)
Enterobacteriaceae_NA_NA (ASV 284)
AClostridia vadinBB60 group_A. hadrus_D. acetoxidans_other (ASV 124)
Clostridia vadinBB60 group_C. gasigens_L. phitofermentans_C. tyrobutyricum_other (ASV 054)
Clostridia vadinBB60 group_F. alocis_C. bacterium_other (ASV 434)
Clostridia vadinBB60 group_A. hadrus_other (ASV 178)
Enterobacteriaceae_NA_NA (ASV 391)
Clostridia vadinBB60 group_F. alocis (ASV 449)
log2 FoldChange
Control EAE
Vancomycin EAE
Ampicillin EAE
E
Muribaculacea (ASV348)
Muribaculacea (ASV363)
Muribaculacea (ASV428)
Muribaculacea (ASV487)
Lachnospiracea (ASV081)
Lachnospiracea (ASV211)
Bacteroides (ASV246)
Relative abundance(%)
Clostridia vadin BB60 (ASV054)
Clostridia vadin BB60 (ASV124)
Clostridia vadin BB60 (ASV178)
Clostridia vadin BB60 (ASV434)
Clostridia vadin BB60 (ASV449)
A. muciniphila ASV231
Enterobacteriacea (ASV284)
EAE
Vancomycin EAE
Ampicillin EAE

Figure 2. Effect of vancomycin on the gut microbiota during the late stage of EAE. Conventionally raised mice were immunized with MOG for EAE induction and starting at day 9 post immunization, mice were treated with vancomycin, ampicillin or vehicle daily for the duration of the experiment. **(A)** Mean clinical EAE scores overtime. Error bars denote mean ± SEM (n = 8 mice/group). Representative data of two independent experiments. Freidman test with Dunn's correction for multiple comparisons. *p< 0.05, **p< 0.01, ***p< 0.001, ****p< 0.0001. **(B)** Principal coordinate analysis of intestinal microbiota samples based on Bray-Curtis showing significantly differently clustering of untreated and antibiotic-treated naïve and EAE mice for all pairwise comparisons in naïve and immunized states (q<0.01). Each dot represents a mouse. **(C)** Taxa plots showing compositional differences in fecal microbiota at the genus level between untreated and antibiotic-treated naïve and EAE mice. **(D)** Species level antibiotic-induced changes in the gut microbiome composition of EAE mice. Results are expressed as log2 fold change, Two-way ANOVA with false discovery rate. All taxa showing significant differences in relative abundance in any pairwise comparisons are shown. **(E)** Relative abundance of selected bacterial species altered in antibiotic treated and untreated EAE mice. Results are presented as mean ± SEM (n = 8 mice/group). Data were analyzed using the Kruskal-Wallis test, followed by Dunn's test for multiple comparisons. *p< 0.05, **p< 0.01, ***p< 0.001, ****p< 0.0001. ASV: amplicon sequence variant

Figure 3

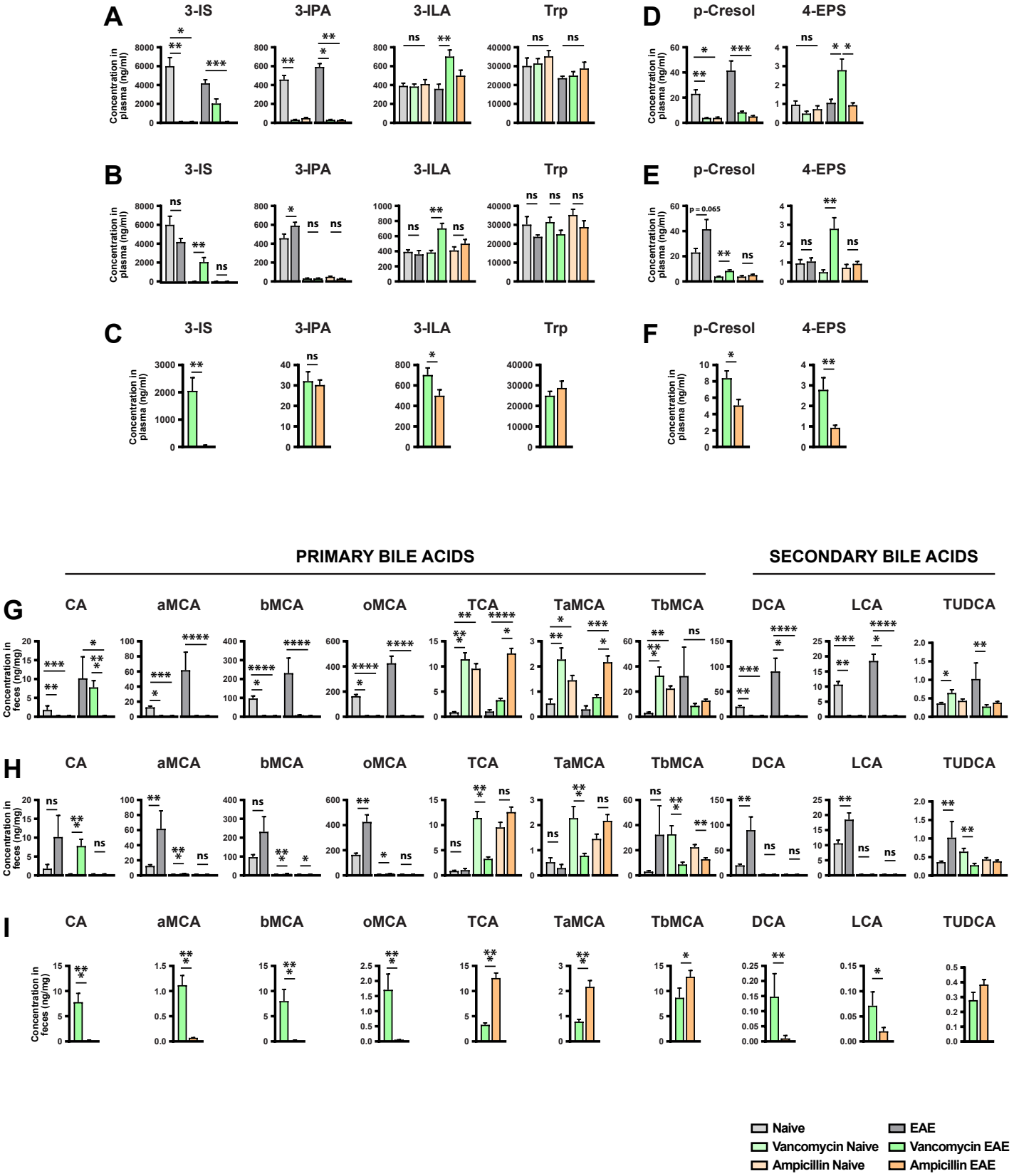
A
3-IS
3-IPA
3-ILA
Trp
D
p-Cresol
4-EPS
B
E
C
F
Concentration in plasma (ng/ml)
p = 0.065
PRIMARY BILE ACIDS
SECONDARY BILE ACIDS
G
H
I
CA
aMCA
bMCA
oMCA
TCA
TaMCA
TbMCA
DCA
LCA
TUDCA
Concentration in feces (ng/mg)
Naive
EAE
Vancomycin Naive
Vancomycin EAE
Ampicillin Naive
Ampicillin EAE

Figure 3. Effect of vancomycin on serum levels of metabolites during the late stage of EAE. Plasma and ceca samples collected from untreated and antibiotic-treated naïve and EAE mice at day 23 post immunization were used for metabolites detection and quantification by liquid chromatography-tandem mass spectrometry. **(A-C)** levels of tryptophan-derived metabolites and **(D-F)** levels of tyrosine-derived metabolites. **(G-I)** levels of bile acids. Results are presented as mean ± SEM (n = 6-8 mice/group). Data were analyzed using the Kruskal-Wallis test with the Dunn's correction (A, B, D, E, G, H, J), or the Mann-Whittney non-parametric test (C, F, I). *$p < 0.05$, **$p < 0.01$, ***$p < 0.001$, ****$p < 0.0001$.

Figure 4

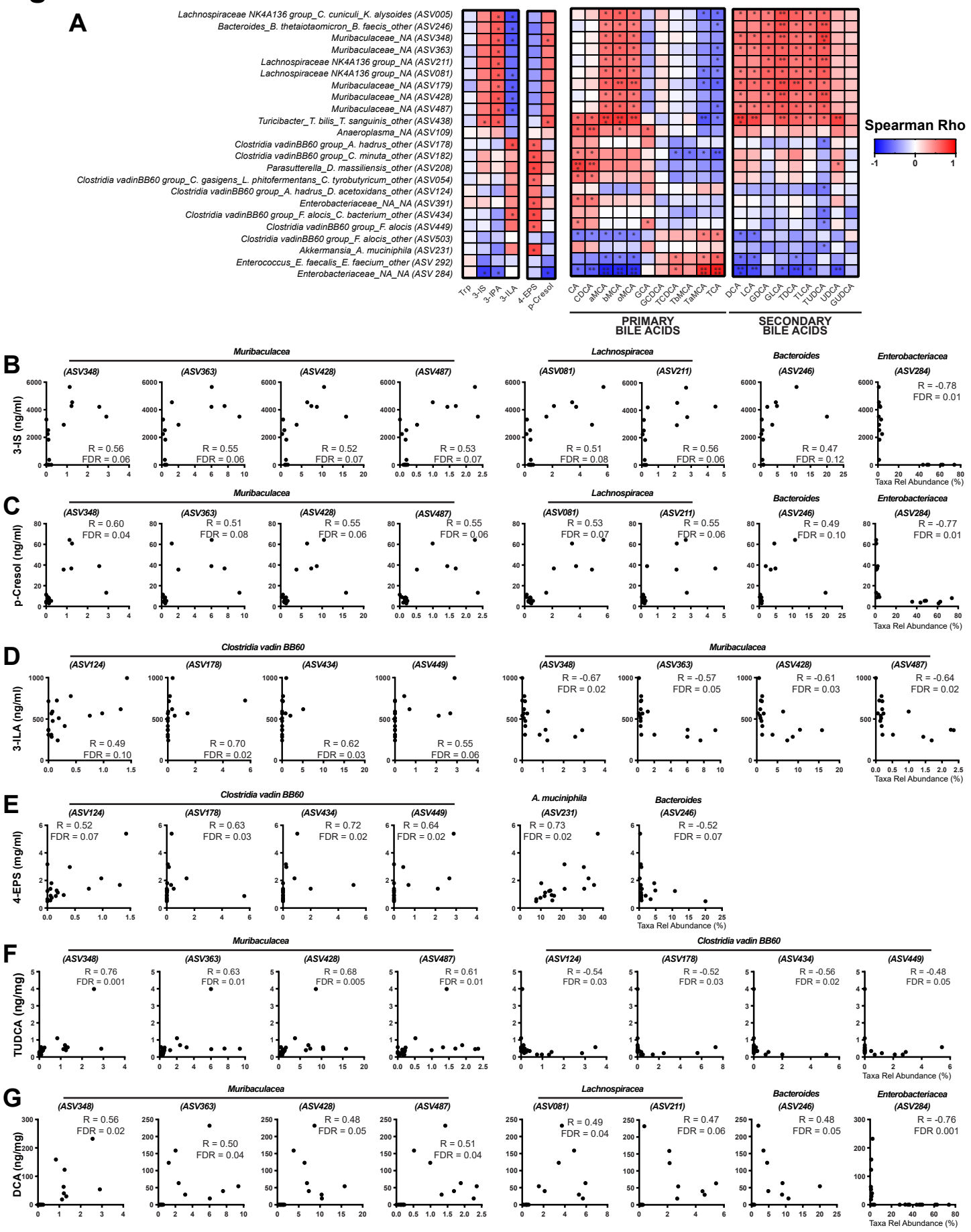
A
Lachnospiraceae NK4A136 group_C. cuniculi_K. alysoides (ASV005)
Bacteroides_B. thetaiotaomicron_B. faecis_other (ASV246)
Muribaculaceae_NA (ASV348)
Muribaculaceae_NA (ASV363)
Lachnospiraceae NK4A136 group_NA (ASV211)
Lachnospiraceae NK4A136 group_NA (ASV081)
Muribaculaceae_NA (ASV179)
Muribaculaceae_NA (ASV428)
Muribaculaceae_NA (ASV487)
Turicibacter_T. bilis_T. sanguinis_other (ASV438)
Anaeroplasma_NA (ASV109)
Clostridia vadinBB60 group_A. hadrus_other (ASV178)
Clostridia vadinBB60 group_C. minuta_other (ASV182)
Parasutterella_D. massiliensis_other (ASV208)
Clostridia vadinBB60 group_C. gasigens_L. phitofermentans_C. tyrobutyricum_other (ASV054)
Clostridia vadinBB60 group_A. hadrus_D. acetoxidans_other (ASV124)
Enterobacteriaceae_NA_NA (ASV391)
Clostridia vadinBB60 group_F. alocis_C. bacterium_other (ASV434)
Clostridia vadinBB60 group_F. alocis (ASV449)
Clostridia vadinBB60 group_F. alocis_other (ASV503)
Akkermansia_A. muciniphila (ASV231)
Enterococcus_E. faecalis_E. faecium_other (ASV 292)
Enterobacteriaceae_NA_NA (ASV 284)
Trp
3-IS
3-IPA
3-ILA
4-EPS
p-Cresol
CA
CDCA
aMCA
bMCA
oMCA
GCA
GCDCA
TCDCA
TbMCA
TaMCA
TCA
DCA
LCA
GDCA
GLCA
TDCA
TLCA
TUDCA
UDCA
GUDCA
PRIMARY BILE ACIDS
SECONDARY BILE ACIDS
Spearman Rho
-1
0
1
B
Muribaculacea
Lachnospiracea
Bacteroides
Enterobacteriacea
(ASV348) R = 0.56 FDR = 0.06
(ASV363) R = 0.55 FDR = 0.06
(ASV428) R = 0.52 FDR = 0.07
(ASV487) R = 0.53 FDR = 0.07
(ASV081) R = 0.51 FDR = 0.08
(ASV211) R = 0.56 FDR = 0.06
(ASV246) R = 0.47 FDR = 0.12
(ASV284) R = -0.78 FDR = 0.01
3-IS (ng/ml)
Taxa Rel Abundance (%)
C
(ASV348) R = 0.60 FDR = 0.04
(ASV363) R = 0.51 FDR = 0.08
(ASV428) R = 0.55 FDR = 0.06
(ASV487) R = 0.55 FDR = 0.06
(ASV081) R = 0.53 FDR = 0.07
(ASV211) R = 0.55 FDR = 0.06
(ASV246) R = 0.49 FDR = 0.10
(ASV284) R = -0.77 FDR = 0.01
p-Cresol (ng/ml)
Taxa Rel Abundance (%)
D
Clostridia vadin BB60
Muribaculacea
(ASV124) R = 0.49 FDR = 0.10
(ASV178) R = 0.70 FDR = 0.02
(ASV434) R = 0.62 FDR = 0.03
(ASV449) R = 0.55 FDR = 0.06
(ASV348) R = -0.67 FDR = 0.02
(ASV363) R = -0.57 FDR = 0.05
(ASV428) R = -0.61 FDR = 0.03
(ASV487) R = -0.64 FDR = 0.02
3-ILA (ng/ml)
Taxa Rel Abundance (%)
E
Clostridia vadin BB60
A. muciniphila
Bacteroides
(ASV124) R = 0.52 FDR = 0.07
(ASV178) R = 0.63 FDR = 0.03
(ASV434) R = 0.72 FDR = 0.02
(ASV449) R = 0.64 FDR = 0.02
(ASV231) R = 0.73 FDR = 0.02
(ASV246) R = -0.52 FDR = 0.07
4-EPS (mg/ml)
Taxa Rel Abundance (%)
F
Muribaculacea
Clostridia vadin BB60
(ASV348) R = 0.76 FDR = 0.001
(ASV363) R = 0.63 FDR = 0.01
(ASV428) R = 0.68 FDR = 0.005
(ASV487) R = 0.61 FDR = 0.01
(ASV124) R = -0.54 FDR = 0.03
(ASV178) R = -0.52 FDR = 0.03
(ASV434) R = -0.56 FDR = 0.02
(ASV449) R = -0.48 FDR = 0.05
TUDCA (ng/mg)
Taxa Rel Abundance (%)
G
Muribaculacea
Lachnospiracea
Bacteroides
Enterobacteriacea
(ASV348) R = 0.56 FDR = 0.02
(ASV363) R = 0.50 FDR = 0.04
(ASV428) R = 0.48 FDR = 0.05
(ASV487) R = 0.51 FDR = 0.04
(ASV081) R = 0.49 FDR = 0.04
(ASV211) R = 0.47 FDR = 0.06
(ASV246) R = 0.48 FDR = 0.05
(ASV284) R = -0.76 FDR 0.001
DCA (ng/mg)
Taxa Rel Abundance (%)

Figure 4. Microbiota associated with metabolites during the late stage of EAE. Spearman's correlation between relative abundance of indicated taxa and metabolites concentrations. **(A)** Correlation matrix of selected taxa at the lowest classifiable levels showing significant correlations (FDR<0.05). *p< 0.05; **p< 0.01; ***p< 0.001; ****p< 0.001. **(B-G)** Scatter plots of selected taxa at the lowest classifiable levels showing significant correlations. ASV: amplicon sequence variant, R: spearman's correlation coefficient.

Figure 5

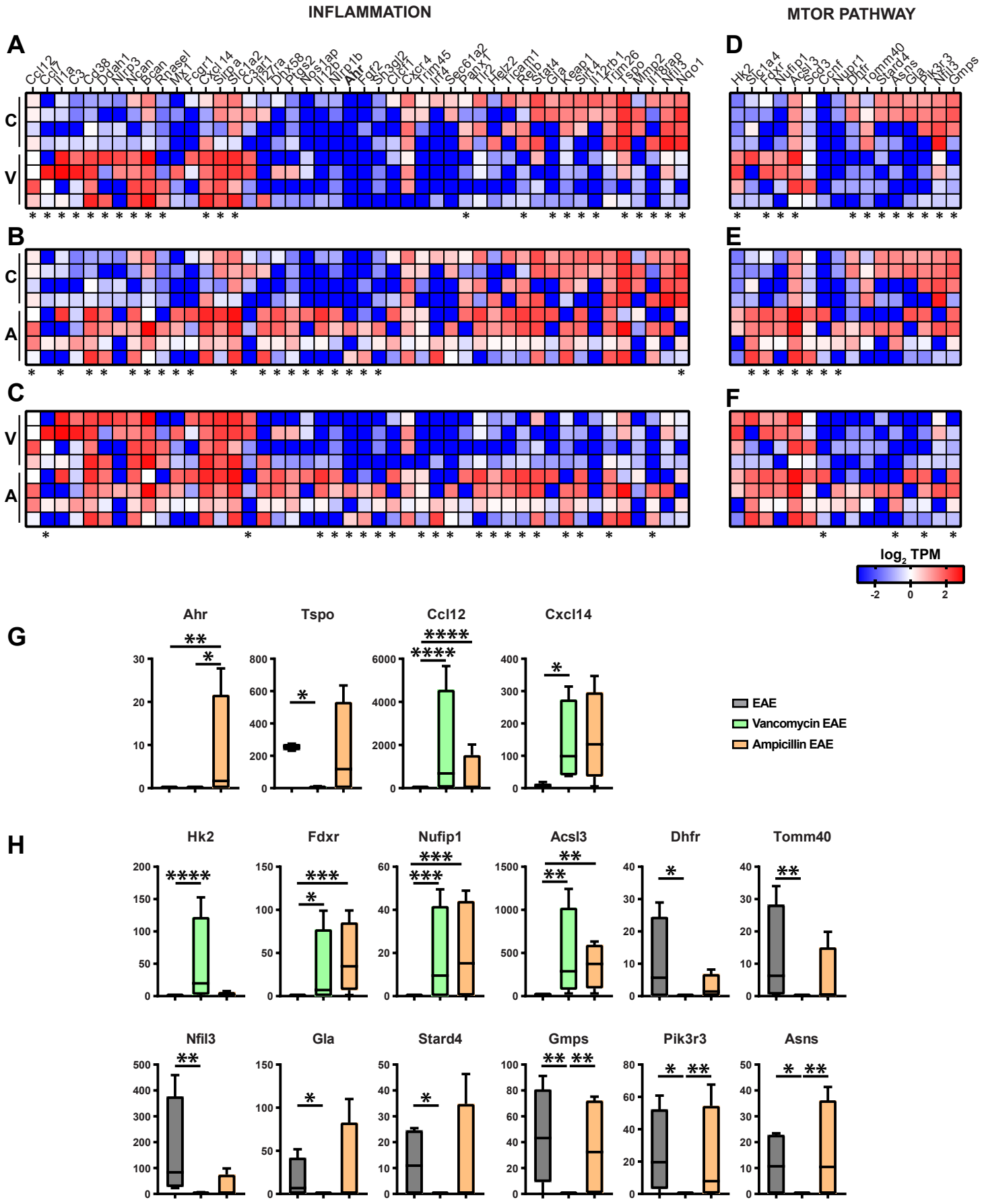
INFLAMMATION
MTOR PATHWAY
A
B
C
D
E
F
G
H
log2 TPM
-2
0
2
EAE
Vancomycin EAE
Ampicillin EAE
Ahr
Tspo
Ccl12
Cxcl14
Hk2
Fdxr
Nufip1
Acsl3
Dhfr
Tomm40
Nfil3
Gla
Stard4
Gmps
Pik3r3
Asns

Figure 5. Vancomycin treatment regulates the expression of genes associated with inflammation and the mTOR pathway in astrocytes during the late stage of EAE. Total RNA was extracted from astrocytes isolated from spinal cords of naïve and EAE mice treated with Vancomycin, Ampicillin or vehicle. Differentially expressed (**A-C**) inflammatory genes and (**D-F**) mTOR pathway genes across treatment groups were identified using DESeq2 and analyzed using the Wald test. Genes with adjusted p-values < 0.05 and absolute log2 fold changes >1 were defined as differentially expressed genes in each pairwise comparison. Individual values are shown (n = 4 mice/group). Results are expressed as log 10 TPM (Transcripts per kilobase million). *p< 0.05, Wald test. **G.** Selected differentially expressed inflammatory genes; *p< 0.05; **p< 0.01; ***p< 0.001. **H.** Differentially expressed mTOR pathway genes; Results are presented as median with interquartile ranges, whiskers represent minimum and maximum values *p< 0.05; **p< 0.01; ***p< 0.001, Wald test.

Figure 6

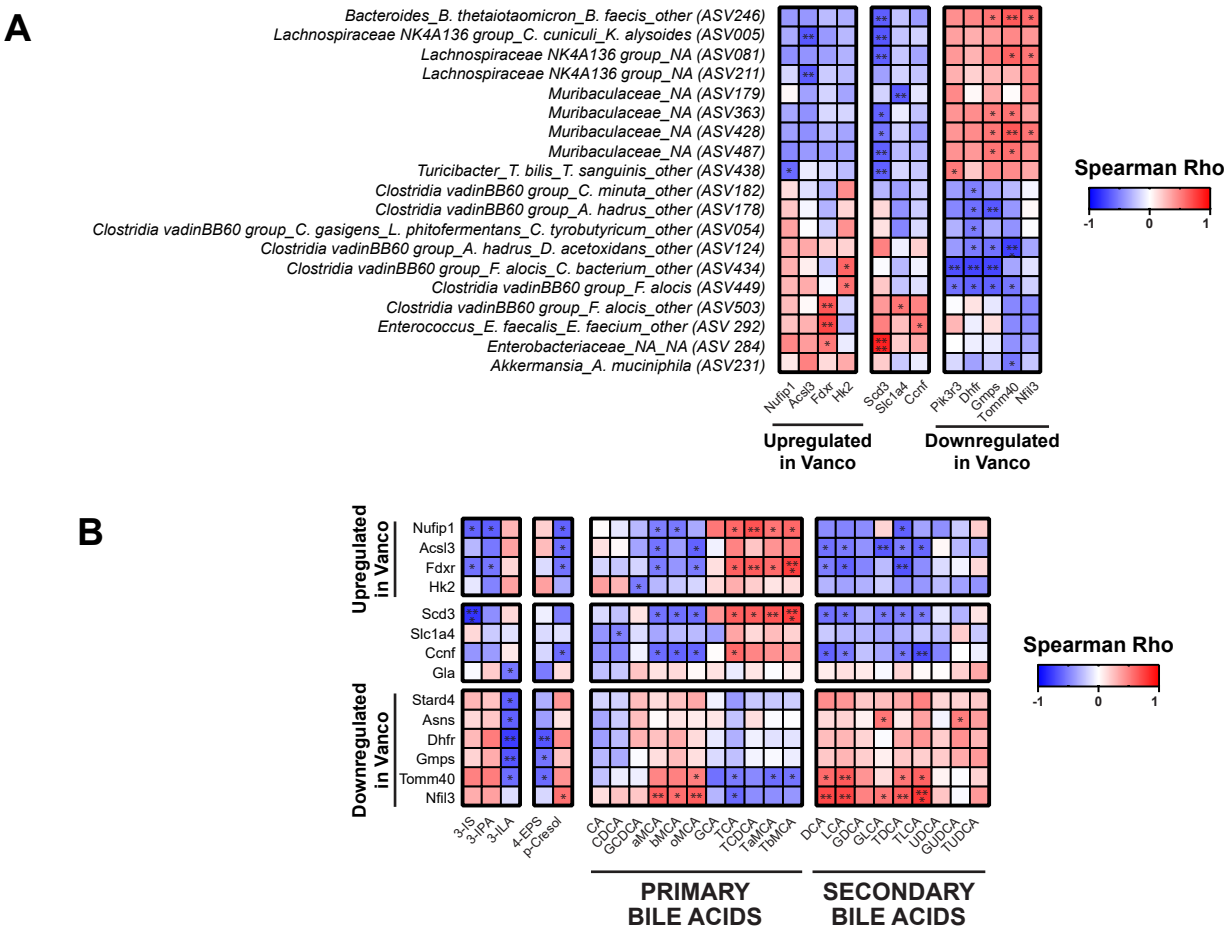
A
Bacteroides_B. thetaiotaomicron_B. faecis_other (ASV246)
Lachnospiraceae NK4A136 group_C. cuniculi_K. alysoides (ASV005)
Lachnospiraceae NK4A136 group_NA (ASV081)
Lachnospiraceae NK4A136 group_NA (ASV211)
Muribaculaceae_NA (ASV179)
Muribaculaceae_NA (ASV363)
Muribaculaceae_NA (ASV428)
Muribaculaceae_NA (ASV487)
Turicibacter_T. bilis_T. sanguinis_other (ASV438)
Clostridia vadinBB60 group_C. minuta_other (ASV182)
Clostridia vadinBB60 group_A. hadrus_other (ASV178)
Clostridia vadinBB60 group_C. gasigens_L. phitofermentans_C. tyrobutyricum_other (ASV054)
Clostridia vadinBB60 group_A. hadrus_D. acetoxidans_other (ASV124)
Clostridia vadinBB60 group_F. alocis_C. bacterium_other (ASV434)
Clostridia vadinBB60 group_F. alocis (ASV449)
Clostridia vadinBB60 group_F. alocis_other (ASV503)
Enterococcus_E. faecalis_E. faecium_other (ASV 292)
Enterobacteriaceae_NA_NA (ASV 284)
Akkermansia_A. muciniphila (ASV231)
Nufip1
Acsl3
Fdxr
Hk2
Scd3
Slc1a4
Ccnf
Plk3r3
Dhfr
Gmps
Tomm40
Nfil3
Upregulated in Vanco
Downregulated in Vanco
Spearman Rho
-1
0
1
B
Upregulated in Vanco
Nufip1
Acsl3
Fdxr
Hk2
Scd3
Slc1a4
Ccnf
Gla
Downregulated in Vanco
Stard4
Asns
Dhfr
Gmps
Tomm40
Nfil3
3-IS
3-IPA
3-ILA
4-EPS
p-Cresol
CA
CDCA
GCDCA
aMCA
bMCA
oMCA
GCA
TCA
TCDCA
TaMCA
TbMCA
DCA
LCA
GDCA
GLCA
TDCA
TLCA
UDCA
GUDCA
TUDCA
PRIMARY BILE ACIDS
SECONDARY BILE ACIDS
Spearman Rho
-1
0
1

Figure 6. Microbiota and metabolites linked with level of expression of mTOR pathway genes in astrocytes during the late stage of EAE. (A) Spearman's correlation between differentially expressed mTOR pathway genes and abundance of selected taxa. **(B)** Spearman's correlation between differentially expressed mTOR pathway genes and metabolite concentrations. *$p < 0.05$; **$p < 0.01$; ***$p < 0.001$; ****$p < 0.001$. Taxa names are indicated at the lowest classifiable level. ASV: amplicon sequence variant.

Figure 7

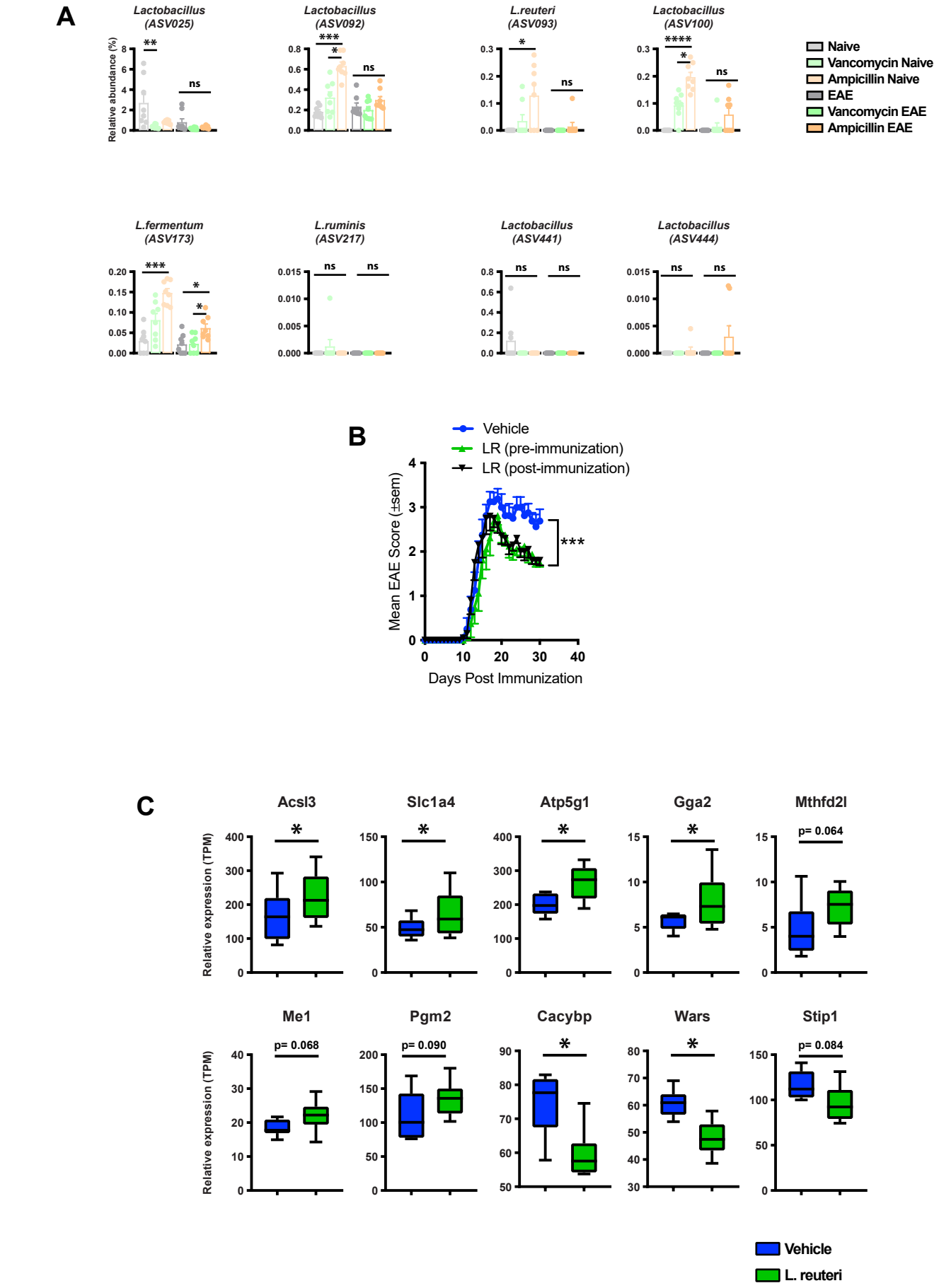
A
Lactobacillus (ASV025)
Lactobacillus (ASV092)
L.reuteri (ASV093)
Lactobacillus (ASV100)
L.fermentum (ASV173)
L.ruminis (ASV217)
Lactobacillus (ASV441)
Lactobacillus (ASV444)
Relative abundance (%)
ns
Naive
Vancomycin Naive
Ampicillin Naive
EAE
Vancomycin EAE
Ampicillin EAE
B
Vehicle
LR (pre-immunization)
LR (post-immunization)
Mean EAE Score (±sem)
Days Post Immunization
C
Acsl3
Slc1a4
Atp5g1
Gga2
Mthfd2l
Me1
Pgm2
Cacybp
Wars
Stip1
Relative expression (TPM)
p= 0.064
p= 0.068
p= 0.090
p= 0.084
Vehicle
L. reuteri

Figure 7*. Lactobacillus reuteri* ameliorates EAE and modulates the expression of the mTOR pathway genes in astrocytes. (A) Relative abundance of eight ASVs belonging to the genus *Lactobacillus* in untreated and antibiotic-treated naïve and EAE mice. Error bars denote mean ± SEM with individual values (n = 8 mice/group). Data were analyzed using Kruskal-Wallis test, followed by Dunn's test for multiple comparisons. Taxa names are indicated at the lowest classifiable level. **(B)** mice were orally gavaged 3-times a week with vehicle (blue), or *Lactobacillus reuteri* starting either 3 weeks before (green), or 15 days after (black) EAE induction, until the end of the experiment. **(B)** Mean EAE clinical scores overtime. Error bars denote mean ±SEM (n=10 mice/group). Representative data of three independent experiments. Data were analyzed using the Freidman test with Dunn's correction for multiple comparisons. **(C)** mTOR pathway genes that are differentially expressed between mice treated with *L. reuteri* and vehicle were identified using DESeq2 and analyzed using the Wald test. Genes with p-values < 0.05 were defined as differentially expressed genes. Results are expressed as TPM (Transcripts per kilobase million). Boxplots show median with interquartile ranges, whiskers represent minimum and maximum values (n = 4-6 mice/group). *p< 0.05, **p< 0.01, ***p< 0.001, ****p< 0.0001, ASV: amplicon sequence variant

Figure 8

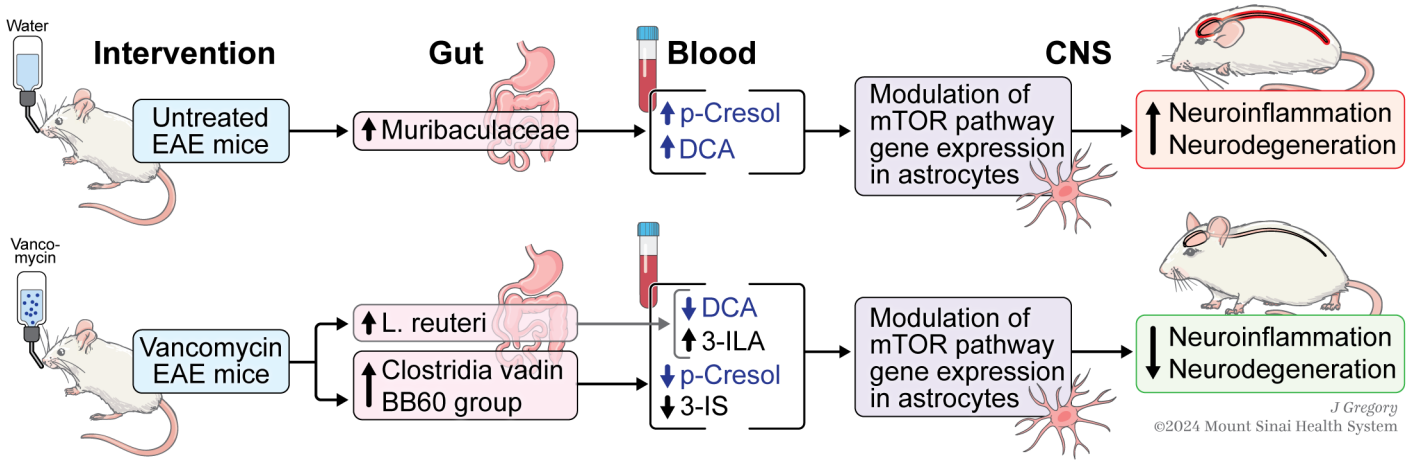
Water
Intervention
Gut
Blood
CNS
Untreated EAE mice
Muribaculaceae
p-Cresol
DCA
Modulation of mTOR pathway gene expression in astrocytes
Neuroinflammation
Neurodegeneration
Vanco-mycin
Vancomycin EAE mice
L. reuteri
Clostridia vadin BB60 group
DCA
3-ILA
p-Cresol
3-IS
Modulation of mTOR pathway gene expression in astrocytes
Neuroinflammation
Neurodegeneration
J Gregory
©2024 Mount Sinai Health System

Figure 8. Hypothesized model diagram for this study. Study summary scheme.

Figure S1

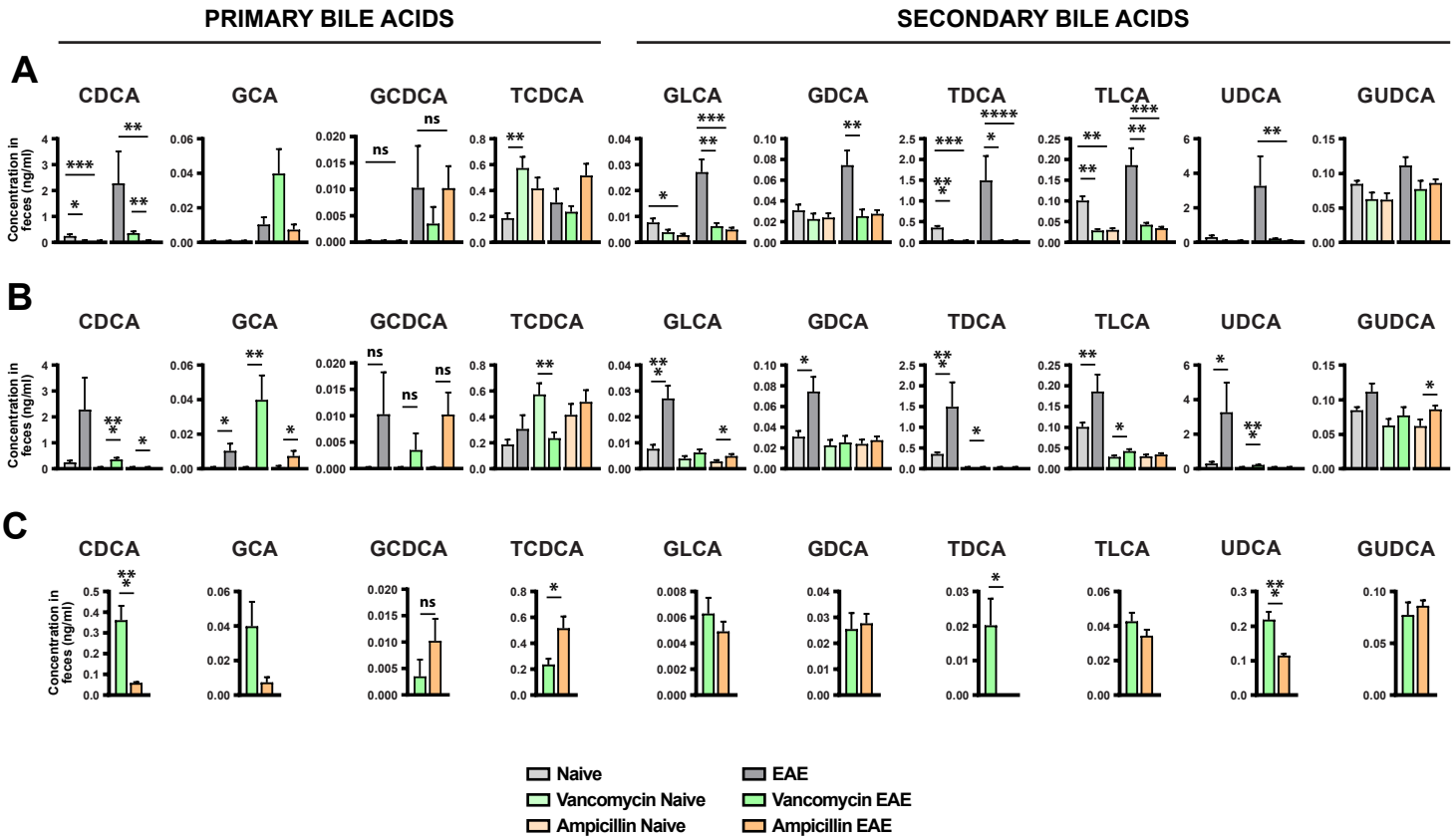
PRIMARY BILE ACIDS
SECONDARY BILE ACIDS
A
B
C
CDCA
GCA
GCDCA
TCDCA
GLCA
GDCA
TDCA
TLCA
UDCA
GUDCA
Concentration in feces (ng/ml)
Naive
Vancomycin Naive
Ampicillin Naive
EAE
Vancomycin EAE
Ampicillin EAE

Supplementary Figure 1. Additional bile acid levels in feces from untreated or antibiotic-treated naïve and EAE mice. (A-C) The concentration of bile acids was measured by liquid chromatography-tandem mass spectrometry in fecal samples. Error bars denote mean ±SEM (n = 8 mice/group). Data were analyzed using the Kruskal-Wallis test with the Dunn's correction (**A, B**), or the Mann-Whittney non-parametric test (**C**). *$p < 0.05$, **$p < 0.01$, ***$p < 0.001$, ****$p < 0.0001$

Figure S2

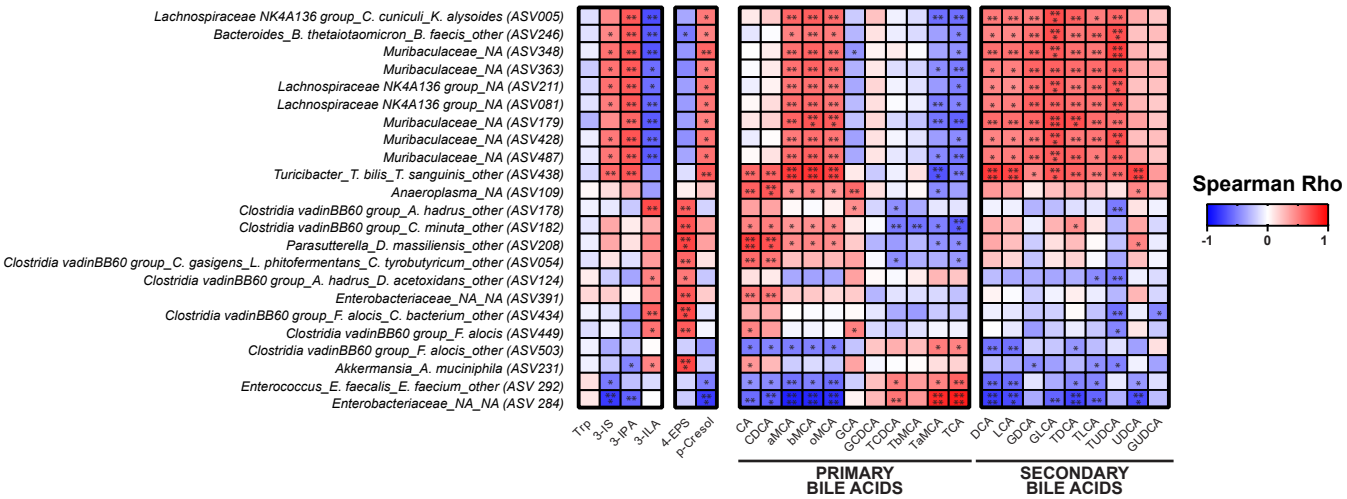
Lachnospiraceae NK4A136 group_C. cuniculi_K. alysoides (ASV005)
Bacteroides_B. thetaiotaomicron_B. faecis_other (ASV246)
Muribaculaceae_NA (ASV348)
Muribaculaceae_NA (ASV363)
Lachnospiraceae NK4A136 group_NA (ASV211)
Lachnospiraceae NK4A136 group_NA (ASV081)
Muribaculaceae_NA (ASV179)
Muribaculaceae_NA (ASV428)
Muribaculaceae_NA (ASV487)
Turicibacter_T. bilis_T. sanguinis_other (ASV438)
Anaeroplasma_NA (ASV109)
Clostridia vadinBB60 group_A. hadrus_other (ASV178)
Clostridia vadinBB60 group_C. minuta_other (ASV182)
Parasutterella_D. massiliensis_other (ASV208)
Clostridia vadinBB60 group_C. gasigens_L. phitofermentans_C. tyrobutyricum_other (ASV054)
Clostridia vadinBB60 group_A. hadrus_D. acetoxidans_other (ASV124)
Enterobacteriaceae_NA_NA (ASV391)
Clostridia vadinBB60 group_F. alocis_C. bacterium_other (ASV434)
Clostridia vadinBB60 group_F. alocis (ASV449)
Clostridia vadinBB60 group_F. alocis_other (ASV503)
Akkermansia_A. muciniphila (ASV231)
Enterococcus_E. faecalis_E. faecium_other (ASV 292)
Enterobacteriaceae_NA_NA (ASV 284)
Trp
3-IS
3-IPA
3-ILA
4-EPS
p-Cresol
CA
CDCA
aMCA
bMCA
oMCA
GCA
GCDCA
TCDCA
TbMCA
TaMCA
TCA
DCA
LCA
GDCA
GLCA
TDCA
TLCA
TUDCA
UDCA
GUDCA
PRIMARY BILE ACIDS
SECONDARY BILE ACIDS
Spearman Rho
-1
0
1

Supplementary Figure 2. Microbiota associated with metabolites during the late stage of EAE. Spearman's correlation between relative abundance of indicated taxa and metabolites concentrations. Correlation matrix of selected taxa at the lowest classifiable levels showing significant correlations (non-adjusted p-values). *p< 0.05; **p< 0.01; ***p< 0.001; ****p< 0.001

Figure S3

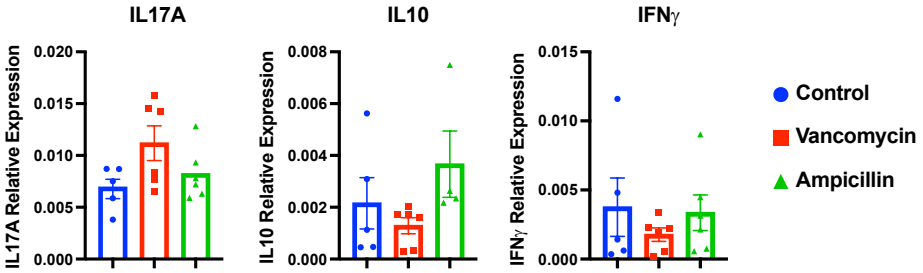
IL17A
IL10
IFNγ
IL17A Relative Expression
IL10 Relative Expression
IFNγ Relative Expression
0.020
0.015
0.010
0.005
0.000
0.008
0.006
0.004
0.002
0.000
0.015
0.010
0.005
0.000
Control
Vancomycin
Ampicillin

Supplementary Figure 3. Cytokines expression in spleen. Relative expression of IL-10, IL-17A and IFN-γ were assessed by qPCR in spleens from untreated EAE mice as well as EAE mice treated with vancomycin or ampicillin. Representative data of two independent experiments. Results were analyzed using one-way ANOVA followed by Bonferroni's multiple comparisons test. Error bars denote mean ±SEM with individual values, ns: not significant.

Figure S4

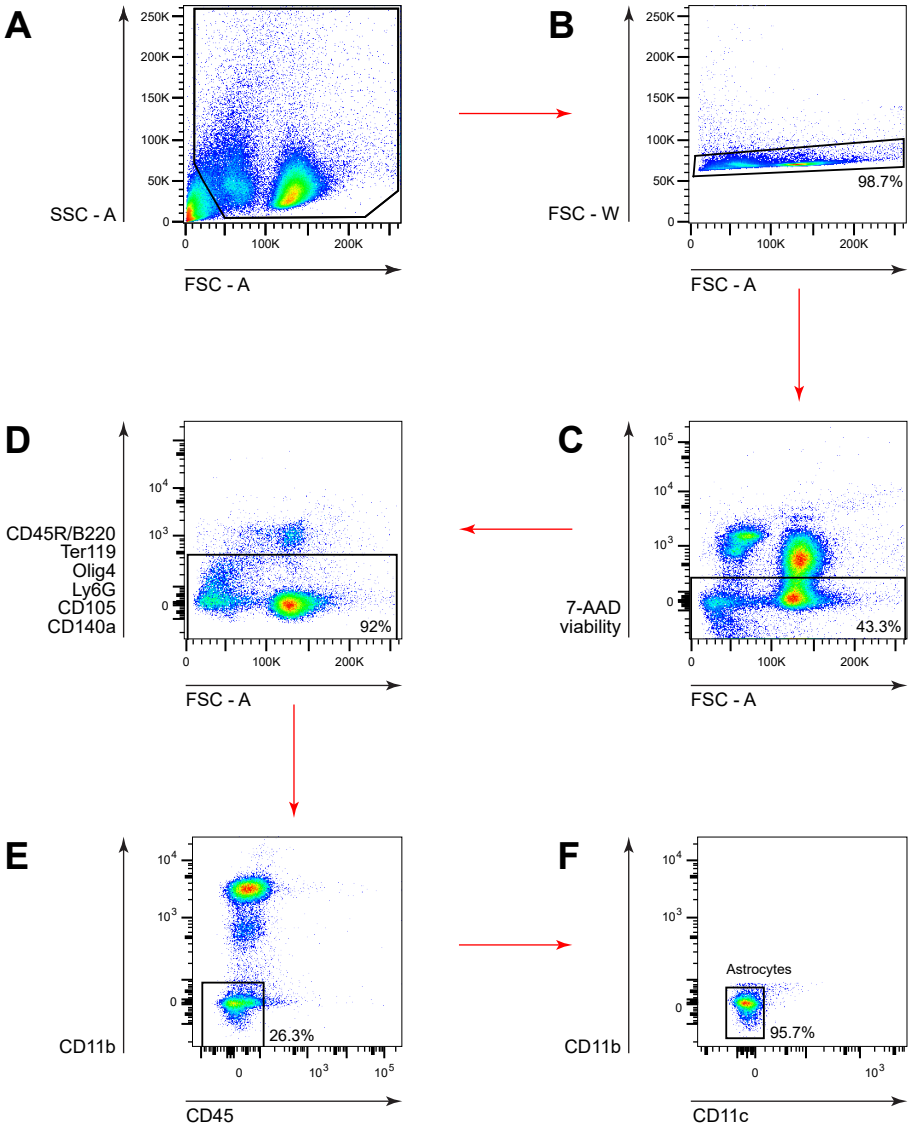
A
SSC - A
FSC - A
B
FSC - W
FSC - A
98.7%
C
7-AAD viability
FSC - A
43.3%
D
CD45R/B220
Ter119
Olig4
Ly6G
CD105
CD140a
FSC - A
92%
E
CD11b
CD45
26.3%
F
CD11b
CD11c
Astrocytes
95.7%

Supplementary Figure 4. FACS gating strategy for astrocytes sorting. **(A)** Mononuclear CNS cells were gated based on SSC-A versus FSC-A and **(B)** singlets were selected from the FSC-A versus FSC-W dot plot. **(C)** Dead cells were excluded with 7-AAD viability dye. **(D)** Cells positive for CD45R/B220 (B cells, T/NK cell subset), Ter119 (erythroid cells), Olig4 (oligodendrocytes), CD105 (endothelial cells), CD140a (mesenchymal cells), Ly6C (monocytes), Ly6G (granulocytes, neutrophils) were excluded. **(E)** Cells positive for CD45 (hematolymphoid cells) and CD11b (myeloid cells) were excluded. **(F)** Astrocytes were identified as double negative for CD11b and CD11c (dendritic cells).

Figure S5

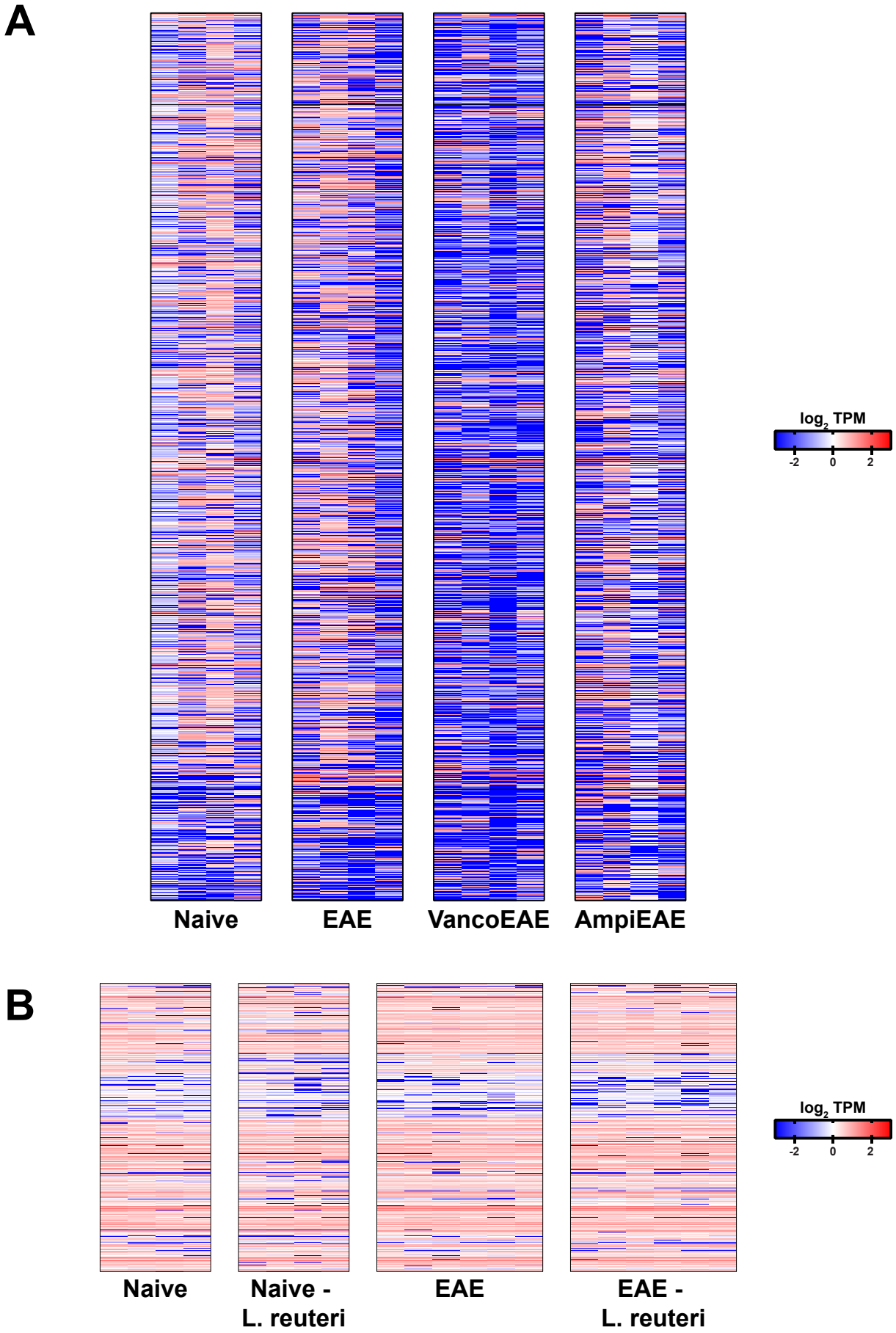
A
Naive
EAE
VancoEAE
AmpiEAE
log2 TPM
-2
0
2
B
Naive
Naive -
L. reuteri
EAE
EAE -
L. reuteri
log2 TPM
-2
0
2

Supplementary Figure 5. Effect of Vancomycin and *Lactobacillus reuteri* on astrocytes transcriptional profile during the late stage of EAE. (A) Heatmaps of 3422 differentially expressed genes in naïve and untreated or antibiotic treated EAE mice. Pairwise comparisons of gene expression between the treatment groups was performed using DESeq2. Expression data was analyzed using the Wald test. Genes with adjusted p-values < 0.05 and absolute log2 fold changes >1 were defined as differentially expressed genes for each pairwise comparison. All genes differentially expressed in any pairwise comparison are included. The color scale represents the log10 (average TPM + 0.01) value. Individual values are shown (n = 4mice/group) **(B)** Heatmaps of 1118 differentially expressed genes between untreated mice and mice colonized with *Lactobacillus reuteri*. Pairwise comparisons of gene expression between the treatment groups were performed using DESeq2. Expression data was analyzed using the Wald test. Genes with p-values < 0.05 were defined as differentially expressed genes for each pairwise comparison. All genes differentially expressed in any pairwise comparison are included. The color scale represents the log10 (average TPM + 0.01) value. TPM: transcripts per kilobase million.